

# 22

## *Quantifying Zooplankton Swimming Behavior: The Question of Scale*

Laurent Seuront, Matthew C. Brewer, and J. Rudi Strickler

### CONTENTS

22.1	Introduction.....	333
22.2	Recording Swimming Paths .....	337
22.2.1	Culture of <i>Daphnia</i> and Algae .....	337
22.2.2	Recording Three-Dimensional Swimming Behavior.....	337
22.3	Characterizing Swimming Paths .....	338
22.3.1	Swimming Path and Fractal Dimension .....	339
22.3.2	Measuring Fractal Dimensions.....	339
22.3.2.1	Compass Method .....	340
22.3.2.2	Box-Counting Method .....	341
22.4	Testing the Robustness of Fractal Dimension Estimates.....	341
22.4.1	On the Scale Dependence of Fractal Dimensions .....	341
22.4.2	Toward an Objective Identification of Scaling Range.....	342
22.4.3	Robustness of Fractal Dimension Estimating Algorithms.....	346
22.4.4	Two-Dimensional vs. Three-Dimensional Fractal Dimension Estimates.....	348
22.5	Comparing Zooplankton Behavior with the Structure of Their Surrounding Environment ....	350
22.6	Conclusion .....	351
	References .....	353

### 22.1 Introduction

Animals typically search for food, hosts, and sexual partners and avoid predators in complex, spatially and temporally structured environments. The resulting movements have implications for the optimization of food search patterns, energy investment, habitat selection, and territorial and social behaviors (Morse, 1980; Pyke, 1984; Stevens and Krebs, 1986; Bell, 1991; Turchin, 1998; Boinski and Garber, 2000). In zooplankton ecology, examples come from the wide spectrum of swimming behaviors related to the species (Tiselius and Jonsson, 1990), the age (Coughlin et al., 1992; van Duren and Videler, 1995; Fisher et al., 2000; Titelman, 2001), the prey density (Tiselius, 1992; Bundy et al., 1993; Dowling et al., 2000), the presence of a predator or a conspecific (van Duren and Videler, 1996; Tiselius et al., 1997; Titelman, 2001), the sex of individuals (van Duren and Videler, 1995; Brewer, 1998; Strickler, 1998), the information imparted into the surrounding water by a swimming animal (Yen and Strickler, 1996; Gries et al., 1999), including both chemical (Yen et al., 1998; Weissburg et al., 1998) and hydromechanical (Costello et al., 1990; Marrasé et al., 1990; Hwang and Strickler, 1994; Hwang et al., 1994; Brewer, 1998) stimuli. Moreover, considering that environmental complexity affects the movement patterns of animals (e.g., Wiens and Milne, 1989; Boinski and Garber, 2000) and the recent advances demonstrating the heterogeneous nature of physical and biological patterns and processes at scales relevant to individual organisms

(Mitchell and Fuhrman, 1989; Squires and Yamazaki, 1995; Cowles et al., 1998; Seuront et al., 1996a, b, 1999), there is a genuine need to establish a reference framework that will link pure behavioral observations, the qualitative and quantitative nature of environment complexity, and zooplankton trophodynamic hypotheses (Turchin, 1991; Keiyu et al., 1994; Seuront, 2001; Seuront et al., 2001; Schmitt and Seuront, 2001, 2002).

Despite the growing number of studies, analyses of the movement patterns of aquatic organisms are still far less common than of terrestrial organisms, primarily because of the difficulty in obtaining accurate records of the displacement of aquatic organisms, which unlike terrestrial organisms, move through a volume and therefore require systems capable of recording three-dimensional (3D) data. This is a nontrivial problem, and has resulted in many investigations of zooplankton behavior recording only two-dimensional (2D) swimming paths. Moreover, even using video systems capable of recording 3D data, there are still problems of scale resulting from the small size of planktonic organisms. Gathering 3D coordinates for zooplankton involves a trade-off between resolution and extent, typically presenting researchers with two alternatives in the collection of data: (1) high spatial resolution, but for short duration, or (2) longer time series, but at low spatial resolution. To our knowledge, the methods used in only four studies have permitted the collection of 3D swimming data at both high spatial resolution and for long periods (Coughlin et al., 1992; Bundy et al., 1993; Brewer, 1996; Schmitt and Seuront, 2001).

Even when the collection of 3D data is possible, behavioral ecologists face another, more fundamental, problem — the accurate quantitative description of animal paths. The difficulty in quantifying animal movement results from the fact that most of the quantitative metrics commonly applied in behavioral studies, e.g., path length, turning angle, turning rate, and net to gross displacement ratio (NGDR), are scale dependent. That is, the metrics will take on different values depending on the physical or temporal scale at which they are measured. This problem was recognized by Dodson et al. (1997), who reported that *Daphnia* swimming speeds were typically two to four times greater when measured at 30 Hz than when measured at 1 Hz. Although they acknowledged the scale dependence of their metrics, they did not propose an objective way to deal with this dilemma. The scale dependence inherent in most metrics results in there being no single scale at which swimming paths can be unambiguously described. Thus, there is no single scale at which swimming behaviors can be compared without leading to arbitrary, potentially spurious conclusions. Furthermore, because individual studies typically record behaviors at different temporal resolutions, (i.e., ranging from 0.01 to 50 Hz; Table 22.1), their results cannot be accurately compared. Despite the clear difficulties associated with scale-dependent metrics, as far as we know only six studies have analyzed plankton swimming behavior in a scale-independent framework (Coughlin et al., 1992; Bundy et al., 1993; Brewer, 1996; Jonsson and Johansson, 1997; Dowling et al., 2000; Schmitt and Seuront, 2001).

Mandelbrot (1977, 1983) introduced the term *fractal* to characterize spatial or temporal phenomena that are continuous but, because of their complexity, not differentiable. Unlike more familiar Euclidean constructs, every attempt to split a fractal into smaller pieces results in the resolution of more structure. As a consequence, in fractal constructs the detail is similar to the whole; i.e., there is no characteristic scale. Fractal objects and processes are therefore said to display “self-invariant” properties (e.g., Hastings and Sugihara, 1993), and can be further defined as being either “self-similar” or “self-affine.” Self-similar objects are isotropic (the same in all three spatial dimensions) upon rescaling, whereas rescaling of self-affine objects is direction dependent (anisotropic). Thus, a trace of zooplankton motion in 3D space is self-similar, whereas a 2D trace, such as the plot of the  $x$ -coordinate of an organism’s movement as a function of time, is self-affine (for more details see Schroeder, 1991). Regardless, fractal analysis presents a new way of addressing questions about structures and scales in ecological systems. In particular, self-invariant patterns and processes can be described by a (non-integer) fractal dimension, which can be viewed as a measure of complexity, or as an index of the scale dependence. The fractal dimension,  $D$ , characterizes a range of scales over which similar patterns and/or processes are operating across that range of scales. However, if there exists a critical scale beyond which a further increase results in a shift in the fractal dimension, or a loss of fractal structure, this may define a transition zone where the environmental properties or constraints acting upon a given system are probably changing rapidly, between two different hierarchical levels in which different patterns and/or processes are operating (Frontier, 1987; Seuront and Lagadeuc, 1997).

TABLE 22.1

Literature Survey of Zooplankton Behavioral Survey, Arranged in Chronological Order

Organism	View	Variable	Metrics [temporal scale]	Ref.
Daphnia	2D, side	Relative light intensity	Speed, position in the water column [-]	Ringelberg (1964)
Cyclops	2D, side	Light	Speed [0.1 Hz]	Strickler (1970)
Daphnia	2D, top	Polarized light	Speed, NGDR, IDT, turning rate [30 Hz]	Wilson and Greaves (1979)
Mesocyclops	2D, top	Prey patches	Speed, loops/min [0.016 Hz]	Williamson (1981)
Daphnia	3D	Angular light distribution	Speed, NGDR [-]	Buchanan et al. (1982)
Daphnia	2D, side	Food concentration	Speed [0.1 Hz]	Porter et al. (1982)
Acartia	2D, top	Bioluminescent dinoflagellates	Speed, NGDR, bursts [15 Hz]	Buskey et al. (1983)
Pseudocalanus	2D, top	Food concentration and odors	Speed, NGDR, bursts, pauses [15 Hz]	Buskey (1984)
Diaptomus	2D, top	Predators and competitors	Speed, NGDR, time between jumps [30 Hz]	Wong et al. (1986)
Daphnia	3D	Food concentration	Speed, turning rate, ground covered [30 Hz]	Young and Getty (1987)
Favella	2D, side	Food patches	Speed, NGDR, turning rate [15 Hz]	Buskey and Stoecker (1988)
Thysanoessa	3D	Algal patches	Speed, NGDR, bursts, % sinking [2 Hz]	Price (1989)
Six calanoids	2D, side	Light, food type	Speed, foraging mode [12.5 Hz]	Tiselius and Jonsson (1990)
Polyphemu	2D, top	Predator-prey interaction	Speed, turning rate, meander [1 Hz]	Young and Taylor (1990)
Bosmina	2D, top	Predator-prey interaction	Speed, turning rate, meander [1 Hz]	Young and Taylor (1990)
Daphnia	3D	Body size	Speed, displacement angle, NGDR, stroke velocity, sinking speed [30 Hz]	Dodson and Ramcharan (1991)
Diaptomus	3D	Predator	Speed, jump length, angle of motion [20 Hz]	Ramcharan and Sprules (1991)
Diaptomus	2D, top	Conspecific	Speed, NGDR [-]	Van Leeuwen and Maly (1991)
Acartia	2D, side	Turbulence	Speed, foraging activity and behavior [25 Hz]	Saiz and Alcaraz (1992)
Amphiprion	3D	Food concentration	Speed, NGDR, turning angles, <b>fractal dimension</b> [10–15 Hz]	Coughlin et al. (1992)
Acartia	2D, side	Food patches	Speed, vertical position, jump frequency, NGDR [0.1 Hz]	Tiselius (1992)
Centropages	3D	Food concentration	Speed, NGDR, Realized Encounter Volume, i.e., <b>fractal dimension</b> [30 Hz]	Bundy et al. (1993)
Various species	2D, side	Species	Speed, NGDR, rate of change in direction [15–30 Hz]	Buskey et al. (1993)
Diaptomus	2D, top	Gravid females	Speed, NGDR [-]	Maly et al. (1994)
Acartia	3D	Food, turbulence	Speed, behavioral observations [30 Hz]	Saiz (1994)
Brachionus	2D, top	Toxic stress	Speed, sinuosity, behavioral observations [25 Hz]	Charoy et al. (1995)
Temora	3D	Food concentration	Speed, NGDR, behavioral observations [50 Hz]	Van Duren and Videler (1995)
Dioithona	2D, side	Light, water flow	Speed, rate of change in directions [30 Hz]	Buskey et al. (1996)
Oithona	2D	Developmental stage	Speed, behavioral observations [30Hz]	Paffenhöfer et al. (1996)
Temora	2D, 3D	Predators, conspecific	Speed, NGDR, behavioral observations [50Hz]	Van Duren and Videler (1996)
Daphnia	3D	Food concentration, light, temperature	Speed, turning angle, turning rate, NGDR, <b>fractal dimension</b> [10Hz]	Brewer (1996)
Daphnia	2D, top	Food concentration	Speed [-]	Larsson and Kleiven (1996)

**TABLE 22.1 (continued)**

Literature Survey of Zooplankton Behavioral Survey, Arranged in Chronological Order

Organism	View	Variable	Metrics [temporal scale]	Ref.
Daphnia	3D	Light, food concentration, vessel size	Speed, turning angle [30 Hz]	Dodson et al. (1997)
Acartia	2D	Predators	Encounter rates [-]	Tiselius et al. (1997)
Euplotes	2D, top	Food patches	Speed, motility, <b>fractal dimension</b> [-]	Jonsson and Johansson (1997)
Protoperidinium	2D, top	Food type	Speed, rate of change of direction, behavioral observations [15 Hz]	Buskey (1997)
Centropages	2D	Turbulence, food concentration	% swimming, swimming behavior, jumps [25 Hz]	Caparroy et al. (1998)
Cyclops	3D	Conspecific	Speed, distance between male and female [60 Hz]	Strickler (1998)
Daphnia	3D	Predators	Speed, turning angle, behavioral observations [30 Hz]	O'Keefe et al. (1998)
Lates calcarifers	2D, top	Food concentration	Pause duration, distance traveled between pauses, travel duration, developmental stage, <b>fractal dimension</b> [25 Hz]	Dowling et al. (2000)
Pomacentrus	1D, side	Age	Speed [-]	Fisher et al. (2000)
Sphaeramia	1D, side	Age	Speed [-]	Fisher et al. (2000)
Amphiprion	1D, side	Age	Speed [-]	Fisher et al. (2000)
Acartia	2D, side	Predator	Speed, reaction distance, jumps [60 Hz]	Suchman (2000)
Acartia	3D, side	Age, predators	Speed, jump directionality, frequency, length, and speed [-]	Titelman (2001)
Temora	3D, side	Age, predators	Speed, jump directionality, frequency, length, and speed [-]	Titelman (2001)
Temora	3D	Female	<b>Multifractal parameters</b> [12.5Hz]	Schmitt and Seuront (2001, 2002)

Note: Values in parentheses are the temporal scale at which the listed metrics are calculated in each study.

Because of its scale-independent nature, in recent years fractal geometry has been used to investigate a surprisingly varied set of phenomena including electrochemical deposition (Mach et al., 1994), the structure of physiological systems such as bronchial trees (Shlesinger and West, 1991) and Hiss–Purkinje cardiac conduction (Goldberger et al., 1985), DNA sequences (Provata and Almirantis, 2000), the growth of bacterial colonies (Tang et al., 2001), taxonomic schemes (Burlando, 1990, 1993), and clusters of galaxies and stars (Wu et al., 1999; Pietronero and Labini, 2000). In addition, Frontier (1987), Sugihara and May (1990), and Seuront (1998) describe numerous possible ecological applications of fractals. Fractals have been used to describe habitat complexity (Bradbury and Reichelt, 1983; Bradbury et al., 1984; Gee and Warwick, 1994a, b), species diversity (Frontier, 1985, 1994), the shape of marine particles (Li et al., 1998), growth processes of benthic fauna (Abraham, 2001), the space–time distribution of phytoplankton biomass (Seuront and Lagadeuc, 1997, 1998), movements of marine invertebrates (Erlandson and Kostylev, 1995) or estuarine vertebrates (Dowling et al., 2000), movements of terrestrial invertebrates (Gautestad and Mysterud, 1993; Wiens et al., 1995), and the search paths of small (Cody, 1971; Pyke, 1981) and large (Siniff and Jenssen, 1969; Van Ballemberghe, 1983; Bascompte and Vilà, 1997) terrestrial vertebrates.

Yet even as the use of fractal dimensions has increased, their reliability for use in the quantification of animal paths has recently been questioned. Turchin (1996, 1998) argued on the basis of a simulated path generated by a correlated random walk that fractal dimensions are themselves scale dependent, varying continuously as a function of scale. Similarly, Tsonis and Elsner (1995) emphasized that scaling regions are subjectively estimated and are often the result of the generic property of the quantity to increase or decrease monotonically as the scale approaches zero, regardless of the geometry of the object (see, e.g., Davenport, Chapter 16, this volume). As a consequence, they proposed a standard procedure for dealing with fractal dimension estimates. Additionally, considering that many analyses of 3D behavior are carried out using 2D data (Table 22.1), we address here the question of whether fractal dimensions estimated from 2D trajectories can be reliably used to estimate the 3D structure of swimming paths.

This comes into question for two conceptually distinct reasons. First, following Mandelbrot (1983), the lower ( $D_f + 1$ ) and upper ( $2D_f$ ) limits of the 3D fractal dimension can be estimated from a 2D of  $D_f$  characterizing the same pattern. However, the broadness of the resulting limits (e.g., if the limits are 2.4 to 2.8) and evidence suggesting that extrapolation to higher dimensions (e.g., from 2D to 3D) is invalid (Roy et al., 1987; Huang and Turcotte, 1989) restrict the reliability of this approach. Second, while swimming organisms move in essence in three dimensions, nothing *a priori* ensures the isotropy of their paths. Anisotropy in swimming can be generated by specific food patterns via patch exploitation strategies (Leising and Franks, 2000; Leising, 2001; Seuront et al., 2001), prey switching behavior (Kiørboe et al., 1996; Caparroy et al., 1998), species-specific behavior (Tiselius and Jonsson, 1990), or the effect of gravity (Strickler, 1982). Path isotropy is nevertheless an absolute requirement for extrapolating 2D to 3D behavior, and therefore must be carefully checked.

Given the increasing use of fractal dimensions in ecology in light of continuing questions regarding their utility, the aims of this chapter are to (1) demonstrate the unreliability of scale-dependent metrics and highlight the advantages of a scale-independent framework to characterize plankton swimming behavior, (2) address, in detail, the proposed limitations of fractal analysis, and (3) introduce an efficient statistical framework that will ensure the existence of a scaling range and the subsequent robustness of fractal dimension estimates. A set of high-resolution 3D trajectories of a common freshwater zooplankter, *Daphnia pulex*, are used throughout the chapter as ecological examples to illustrate the concepts presented.

## 22.2 Recording Swimming Paths

Gathering 3D coordinates remains the first (and major) limitation for *in vitro* zooplankton behavioral studies because it entails collection of 3D swimming data both at high spatial resolution and for extended periods of time. From the few studies available in the literature (see, e.g., Coughlin et al., 1992; Bundy et al., 1993; Schmitt and Seuront, 2001), it can nevertheless be seen that the methods used are conceptually similar to the one introduced below.

### 22.2.1 Culture of *Daphnia* and Algae

A clone of *D. pulex* was cultured in aged tap water under cool white fluorescent bulbs, in a 16/8 light–dark cycle. The cultures were maintained at the experimental temperature (20°C) and fed every day with a 1:1 mixture of the green algae *Ankistrodesmus* sp. and *Scenedesmus* sp. at a final concentration of about  $5 \times 10^5$  cells ml<sup>-1</sup>. Algae were grown in multiple 250 ml batch cultures under cool white fluorescent bulbs, in an 18/6 light–dark cycle, at 20°C, in Bold's Basal Medium.

### 22.2.2 Recording Three-Dimensional Swimming Behavior

All paths analyzed in this chapter are the movements of solitary *D. pulex* swimming in the 5-l (18 × 18 × 15.5 cm high) Plexiglas recording vessel of the CritterSpy™, a high-resolution 3D recording system. All recordings were made with animals swimming in an algal concentration of  $5 \times 10^4$  cells ml<sup>-1</sup>, which is an intermediate food concentration, well below *D. pulex*'s incipient limiting concentration (Lampert, 1987). The test chamber was illuminated with a diffused, fiber-optic light placed 0.5 m directly overhead that resulted in an illumination of about 12 μEm<sup>-2</sup> s<sup>-1</sup> in the vessel, approximately equal to full daylight. At least 1 h prior to experiments, adult, gravid females  $2.1 \pm 0.2$  (mm) were transferred from their culturing vessels and acclimated to experimental light and food conditions in holding vessels. A single animal was then transferred from its holding vessel to the recording chamber with a large-bore pipette and allowed to acclimate for at least 10 min before recording began.

The CritterSpy uses a Schleiern optical system consisting of a collimated red laser beam ( $\lambda = 623$  nm) which serves as the light source for two orthogonally mounted video cameras, two frame number generators, two 20-in. video monitors, and two VHS videocassette recorders; see Strickler (1985) and Bundy et al. (1993) for further details. This system simultaneously records orthogonal front (XZ) and side (YZ) views of the experimental chamber as dark field images. To run the system, two operators

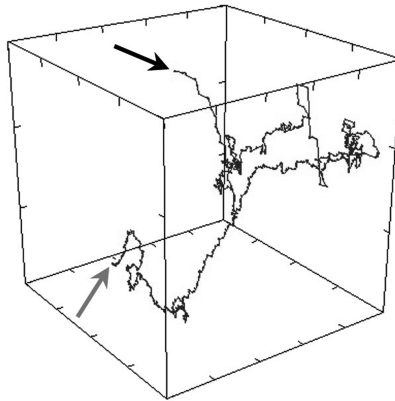


**FIGURE 22.1** Example of a 3D pathway of *D. pulex*. Path is shown to scale in the CritterSpy's 5-l recording vessel.

view the camera images in real time. As the animal swam away from the center of the other camera's view (marked with crosshairs on the monitors), one operator used a trackball (X and Z dimensions) and the other a rotating cylinder (Y dimension) to bring the animal back into the center of both views. The actual recentering of the image was achieved via three computer-controlled linear positioning motors (one for each axis) that moved the entire optical system in response to the operators' input. A computer recorded the motor movements necessary to keep the animal centered in the two views as X, Y, and Z coordinates. Because the computer only recorded coordinates when the trackball or cylinder were moved, the coordinates were recorded at an uneven sampling rate (ranging from about 5 to 15 Hz). Paths were then interpolated to produce an even time interval (10 Hz) between successive position measurements. The 10 Hz rate is rapid enough that coordinates recorded at that temporal scale are the result of very small movements of the crosshairs corresponding to *Daphnia*'s characteristic hop-and-sink behavior.

Each individual *Daphnia* was recorded swimming for at least 30 min, after which the videotapes were reviewed and valid segments were identified for analysis. Valid segments consisted of video in which the animals were swimming freely, at least two body lengths away from any of the chamber's walls or the surface, and the animals were always within one half body length of the crosshairs in the center of the video monitors. To ensure that there would be a significant range of scales in each path, we only used paths that were at least 30 s in duration. After identifying valid sequences, the frame numbers imprinted on the video were used to isolate the corresponding time interval from the 3D coordinate data stored on the computer. These time series of coordinates formed the 3D trajectories used in our analysis (Figure 22.1).

### 22.3 Characterizing Swimming Paths

Movement paths may be characterized by a variety of measures (Figure 22.2; Table 22.1), including: path length (the total distance traveled, or gross displacement), move length (the distance traveled between consecutive points in time), move duration (time interval between successive pauses, as well as between successive spatial points), speed (move length divided by move duration), turning angle (the difference in direction between two successive moves), turning rate (turning angle divided by move duration), net displacement (the linear distance between starting and ending point, often used as a metric when making comparisons with diffusion or correlated random walk models; e.g., Kareiva and Shigesada, 1983; McCulloch and Cain, 1989; Turchin, 1991; Johnson et al., 1992a), NGDR (net to gross displacement ratio; Wilson and Greaves, 1979), and fractal dimension. For paths recorded at fixed time intervals, move duration is a constant. As discussed above, the values of all the metrics except fractal dimension (see below) are implicitly a function of their measurement scale (Figure 22.2). The scale dependence of these ratio metrics, i.e., the path length and the turning angle (Figure 22.3), implies that there is no single scale at which swimming paths can be unambiguously described.

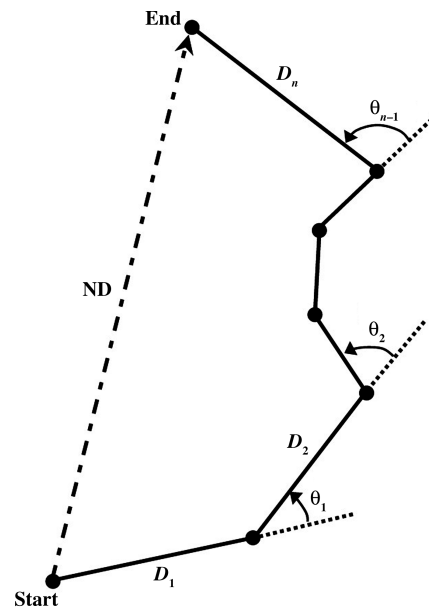


**FIGURE 22.2** Illustration of the different metrics used in characterizing movement pathways. The mean displacement is the mean of distances  $D_i$  traveled per time interval, the net displacement ND is the straight-line distance between the initial and final locations, and the growth displacement is the sum of the distances  $D_i$ . The mean turning angle is the trigonometric mean of angles  $\theta_i$  formed by changes in direction between steps.

### 22.3.1 Swimming Path and Fractal Dimension

Fractal analysis of animal behavior is based on the premise that the fractal dimension can serve as a scale-independent descriptor of the path an organism takes as it moves. The philosophy behind fractals is as follows: if an organism moves along a completely linear path, then the actual distance traveled,  $L$ , equals the displacement between the start and the finish,  $\delta$ . The relationship between these two variables is linear. In other words, if we assume a power law relating  $L$  to  $\delta$ , i.e.,  $L^D = \delta$ , then the exponent  $D = 1$ . According to this power law, if the path deviates from linearity, that is, becomes tortuous, the exponent will then be greater than 1. In the extreme example of “curviness,” i.e., for the case of Brownian motion,  $D = 2$  (Mandelbrot, 1983). It appears that  $D$  provides a measure of the path “tortuosity,” or “complexity,” with the extreme cases delineated by linear and Brownian movement, respectively, and real-life cases expected to fall between these extremes of  $D = 1$  and  $D = 2$ .

We reiterate Turchin et al.’s (1991) position on the importance of using individual organisms, and not steps within an individual path, as statistical replicates. Analyses performed on the above measures are termed second-order statistics because they collapse information from many observations of an individual into a single measure (Batschelet, 1981). In addition, we suggest that strict limits be placed on the minimum number of moves used to obtain a statistic for a given trajectory. Specifically, the minimum number of observed moves should set the number of observed moves from which statistics are gathered from any of the paths.

### 22.3.2 Measuring Fractal Dimensions

Practical approaches to measuring  $D$  using real data have not yet been standardized (e.g., Hastings and Sugihara, 1993). Some investigators plot the net squared displacement as a function of time (Johnson et al., 1992a), a practice that has a solid basis in random walk theory (see, e.g., Tarafdar et al., 2001). Others construct plots of the apparent path length vs. ruler length (With, 1994a). Here, as recommended by Fielding (1992) and Hastings and Sugihara (1993) to ensure the reliability of the fractal dimension estimates, we used two different, but conceptually similar, methods.

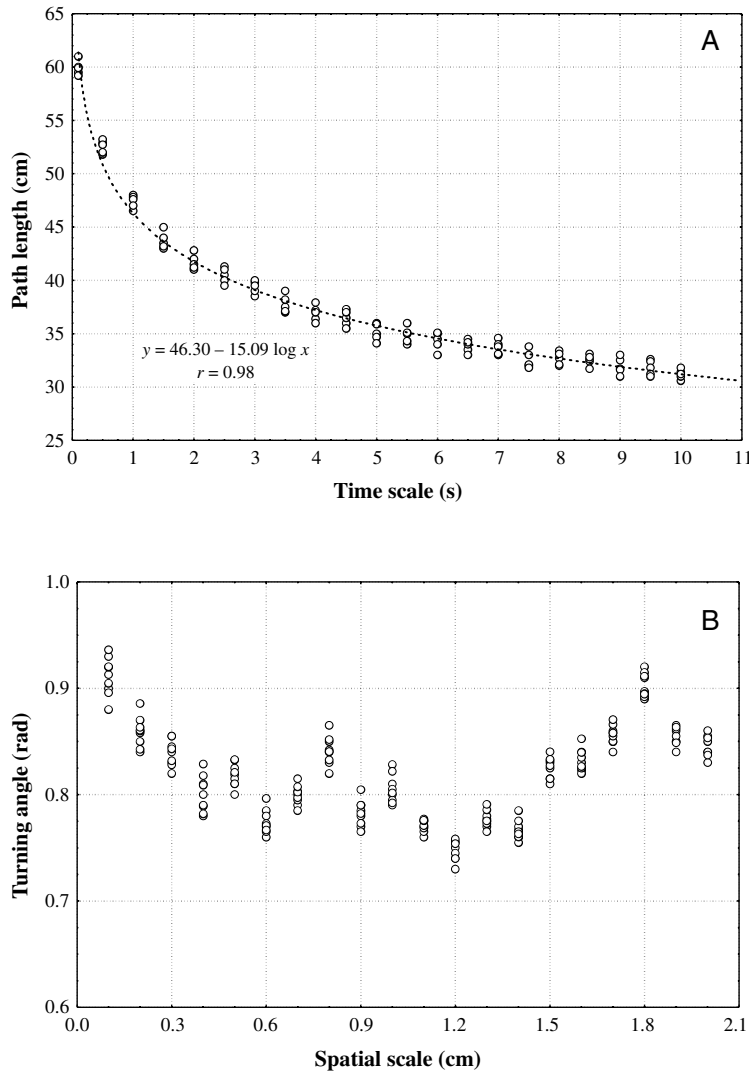


FIGURE 22.3 Scale dependence of path length (A) and turning angle (B) obtained from a 3D swimming path of *D. pulex*.

**22.3.2.1 Compass Method** — Using this procedure, the fractal dimension  $D_c$  is estimated by measuring the length  $L$  of a path at various scale values  $\delta$ . The procedure is analogous to moving a set of dividers (like a drawing compass) of fixed length  $\delta$  along the path (Figure 22.4A). The estimated length of the path is the product of  $N$  (number of compass dividers required to “cover” the object) and the scale factor  $\delta$ . The number of dividers necessary to cover the object then increases with decreasing measurement scale, giving rise to the power law relationship:

$$L(\delta) = k_1 \delta^m \quad (22.1)$$

where  $\delta$  is the measurement scale,  $L(\delta)$  is the measured length of the path,  $L(\delta) = N\delta$ , and  $k_1$  is a constant. Practically, the fractal dimension  $D_c$  is estimated from the slope  $m$  of the log–log plot of  $L(\delta)$  vs.  $\delta$  for various values of  $\delta$ , where

$$D_c = 1 - m \quad (22.2)$$

Hereafter, the fractal dimension  $D_c$  will be referred to as the “compass dimension.”

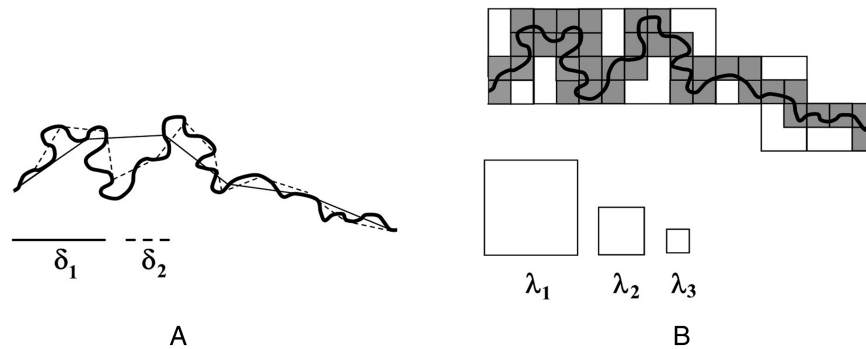


**FIGURE 22.4** 2D illustration of the compass (A) and the box-counting (B) methods used to describe swimming path complexity with fractal dimension. Two steps of the analyses are shown, using two different characteristic scales: the divider lengths  $\delta_1$  and  $\delta_2$ , and the box sizes  $\lambda_1$ ,  $\lambda_2$ , and  $\lambda_3$ .

**22.3.2.2 Box-Counting Method** — This procedure, like the compass method, can be used to measure the fractal dimension of a curve (Longley and Batty, 1989). In addition, it can be applied to overlapping curves (Peitgen et al., 1992) and structures lacking strict self-similar properties such as vegetation (Morse et al., 1985). Formally, the method finds the “ $\lambda$  cover” of the object, i.e., the number of pixels of length  $\lambda$  (or circles of radius  $\lambda$ ) required to cover the object (Voss, 1988). A more practical alternative is to superimpose a regular grid of pixels of length  $\lambda$  on the object and count the number of “occupied” pixels (Figure 22.4B). This procedure is repeated using different values of  $\lambda$ . The volume occupied by a path is then estimated with a series of counting boxes spanning a range of volumes down to some small fraction of the entire volume (Figure 22.4B). The number of occupied boxes increases with decreasing box size, leading to the following power law relationship (Loehle, 1990):

$$N(\lambda) = k_2 \lambda^{-D_b} \quad (22.3)$$

where  $\lambda$  is the box size,  $N(\lambda)$  is the number of boxes occupied by the path,  $k_2$  is a constant, and  $D_b$  is the box-counting fractal dimension, referred to hereafter as the “box dimension.”  $D_b$  is estimated from the slope of the linear trend of the log–log plot of  $N(\lambda)$  vs.  $\lambda$ .

The fractal dimension of a data set is thus measured by making sure that the data have large scale-independent characteristics.

## 22.4 Testing the Robustness of Fractal Dimension Estimates

### 22.4.1 On the Scale Dependence of Fractal Dimensions

Generally, the key assumption regarding the fractal dimension is that it is a scale-independent parameter. Strictly speaking, this means that, in a particular environment, if we calculate  $D$  for the swimming behavior of an organism based on paths that are several centimeters long, we will arrive at the same value of  $D$  for paths measured at a scale of meters to hundreds of meters. This is central to one of the main issues faced by landscape ecologists; understanding how to meaningfully extrapolate ecological information across spatial scales (Gardner et al., 1989; Turner and Gardner, 1991). This scale-independence issue has been addressed in detail by Turchin (1996) who argued, based on a simulated path of 10,000 steps generated by a correlated random walk, that the fractal dimension, rather than being scale invariant, instead varies in a curvilinear fashion from  $D = 1$  at very small spatial scales, to  $D = 2$  at very large spatial scales (see also Davenport, Chapter 16, this volume; his Figure 16.1). However, we propose that these two features are simply artifacts of the algorithms used to estimate dimensions and can be explained accordingly. Because of the limited number of data points as the measurement scale approaches the resolution of the data, the path becomes more and more linear, and thus  $D \rightarrow 1$ . Alternatively, at larger scales most, if not all, of the available boxes have a high probability of including a portion of the path,

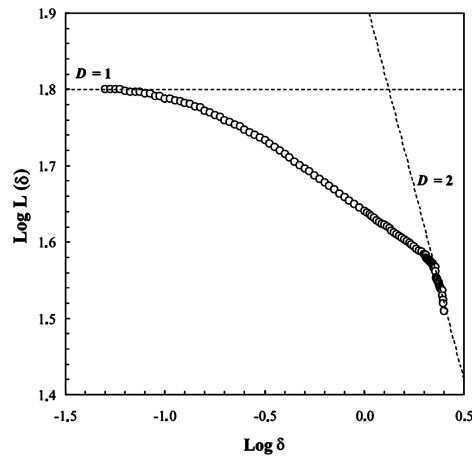


**FIGURE 22.5** Illustration of the behavior of  $L(\delta)$  vs.  $\delta$  in a log–log plot, obtained from a simulated path of 10,000 steps resulting from a correlated random walk (thick dashed line), and from a 3D swimming path of *D. pulex*. Correlated random walks have been simulated following Keiyu et al. (1994).

and thus  $D \rightarrow 2$ . Such behavior is also found in a log–log plot of  $L(\delta)$  vs.  $\delta$  obtained from a 3D path of *D. pulex* (Figure 22.5). This path exhibits the same transition from  $D = 1$  at small scales to  $D = 2$  at larger scales. One must nevertheless note here that the swimming path of *D. pulex* clearly exhibits a linear (i.e., fractal) behavior over intermediate scales, contrary to the Turchin's path generated by a correlated random walk. Moreover, we raised here against Turchin's arguments that while both random walks and correlated random walks have been widely used to model animal behavior (e.g., Johnson and Milne, 1992; Tiselius et al., 1993; Wiens et al., 1993; Gautestad and Mysterud, 1993; Keiyu et al., 1994; Turchin, 1996), they mimic animal paths very poorly (Bergman et al., 2000) because they incorporate an unrealistic arbitrary distribution for the angles between successive steps. A reasonable alternative might be the inclusion of a turning angle distribution, which enables the explicit computation of the effect of persistence in the direction of travel on the expected magnitude of net displacement of the animal over time (e.g., Wu et al., 2000).

On the other hand, because different scales are often associated with different driving processes (e.g., Wiens, 1989; Seuront and Lagadeuc, 1997) the fractal dimension may have the desirable feature of being constant only over a finite, instead of an infinite, range of measurement scales. It is then useful for (1) identifying characteristic scales of variability and (2) comparing movements of organisms that may respond, for example, to the patchy structure of their environment at different absolute scales. Changes in the value of  $D$  with scale may indicate that a new set of environmental or behavioral processes is controlling movement behavior (e.g., decreased influence of patch barriers or the effect of home range behavior). Thus, the scale dependence of the fractal dimension over finite ranges of scales may carry more information, both in terms of driving processes and sampling limitation, than its scale independence over a hypothetical infinite range of scales. Alternatively, although the point of slope change may indicate the operational scale of different generative processes, it may simply reflect the limited spatial resolution of the data being analyzed (Hamilton et al., 1992; Kenkel and Walker, 1993; Gautestad and Mysterud, 1994). However, as previously shown from *D. pulex* trajectory, the effect of spatial resolution in the data will manifest as gradual changes of the fractal dimensions toward  $D \rightarrow 1$  or  $D \rightarrow 2$ , and cannot be confused with a transition zone between two different scaling regions. What is critical for a proper interpretation of fractal dimensions is then a way to identify the range of scales over which fractal dimension is invariant.

#### 22.4.2 Toward an Objective Identification of Scaling Range

When we are dealing with exact fractals (e.g., Koch snowflakes, the Sierpinski carpet; see Schroeder [1991] for further details), there are no difficulties in calculating a fractal dimension. The log–log plots

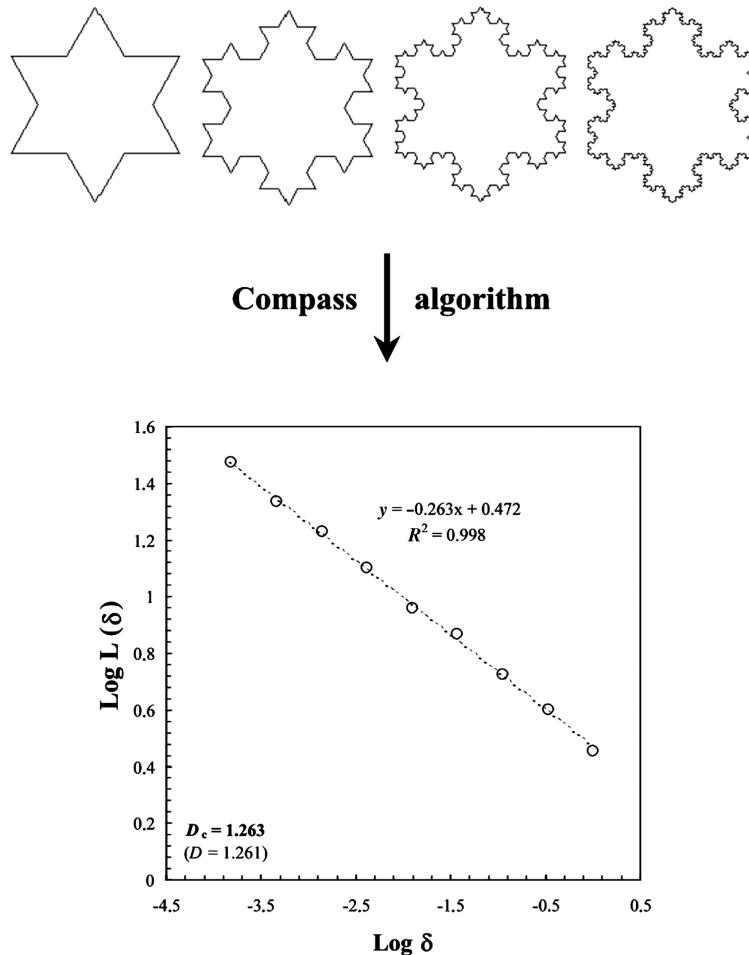


**FIGURE 22.6** Illustration of the behavior of  $L(\delta)$  vs.  $\delta$  in a log–log plot (compass method), obtained from the “Koch snowflake.” The Koch snowflake is a theoretical fractal object obtained by dividing a given segment into four subsegments three times smaller between two steps of the generation process. The expected fractal dimension is then  $D = \log 4 / \log 3 = 1.261$  (Mandelbrot, 1983), and cannot be regarded as being significantly different from the empirical compass dimension  $D_c = 1.268$  given in parentheses ( $p < 0.01$ ). Note the unambiguous linearity of the behavior of  $\log L(\delta)$  vs.  $\log \delta$  over the whole range of available scales, when compared with Figure 22.5.

are very linear and we always recover an *a priori* known result (Figure 22.6 and Figure 22.7). Conversely, when we are dealing with objects or observables from nature whose properties are not known *a priori* (e.g., coastlines, swimming paths), complications begin to arise. In such cases, many analyses have implicitly made an assumption of linearity in the log–log plot (Crist et al., 1992; With, 1994a; Erlandson and Kostylev, 1995; Dowling et al., 2000) and as a result, the scaling region was estimated subjectively. However, as stated above, the apparent scaling can be simply the result of the generic property of the quantity to increase or decrease monotonically as the scale goes to zero irrespective of the geometry of the object. Consequently, one must question the validity of fitting a straight line over the whole range of available scales. We therefore propose here an objective, statistically sound procedure for testing the existence of scaling properties in animal paths.

First, consider a regression window of a varying width that ranges from a minimum of five data points (the least number of data points to ensure the statistical relevance of a regression analysis) to the entire data set. The smallest windows are slid along the entire data set at 0.01 cm (half body length of recorded *Daphnia* individuals) increments, with the whole procedure iterated ( $n - 4$ ) times, where  $n$  is the total number of available data points. Within each window and for each width, we estimate the coefficient of

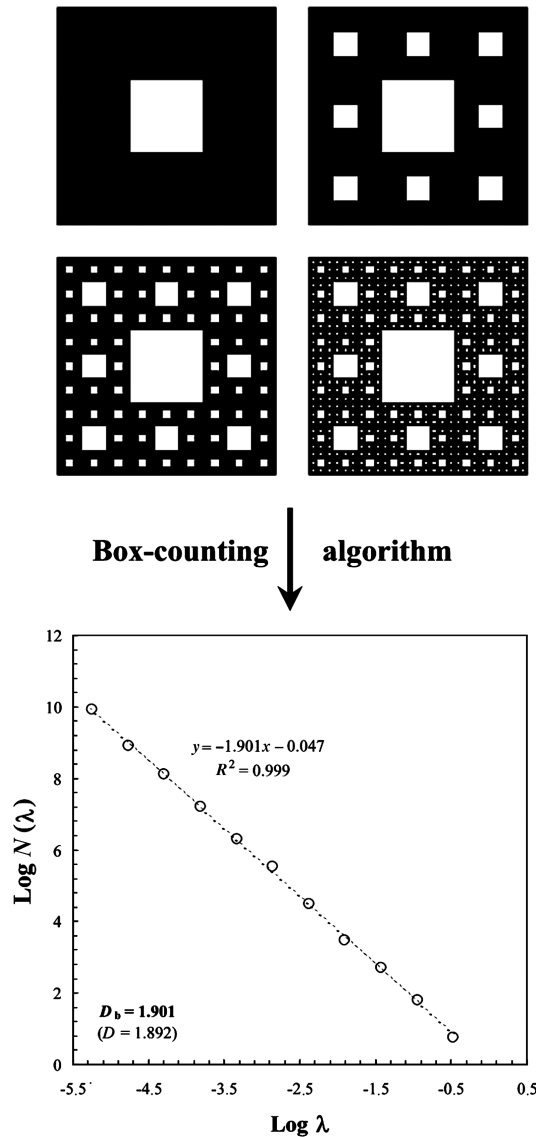


**FIGURE 22.7** Illustration of the behavior of  $N(\lambda)$  vs.  $\lambda$  in a log–log plot (box-counting method), obtained from the “Sierpinski carpet.” The Sierpinski carpet is a theoretical fractal object obtained by dividing a given square into eight subsquares three times smaller between two steps of the generation process. The expected fractal dimension is then  $D = \log 8 / \log 3 = 1.892$ , and cannot be distinguished from the empirical box dimension  $D_b = 1.901$  given in parentheses ( $p < 0.01$ ). Note the unambiguous linearity of the behavior of  $\log N(\lambda)$  vs.  $\log \lambda$  over the whole range of available scales, when compared with Figure 22.5.

determination ( $r^2$ ) and the sum of the squared residuals (SSR) for the regression. Finally, we use the values of  $\delta$  (Equation 22.1) and  $\lambda$  (Equation 22.2), which maximize the coefficient of determination and minimize the total sum of the squared residuals (Seuront and Lagadeuc, 1997) to define the scaling range and to estimate the related fractal dimensions (Figure 22.8A). Hereafter, this first optimization procedure will be referred to as the “ $R^2 - SSR$ ” criterion.

Second, one may note that Equations 22.1 and 22.3 can be rewritten, respectively, as

$$d \log L(\delta) / d \log \delta = 1 - D_c \quad (22.4)$$

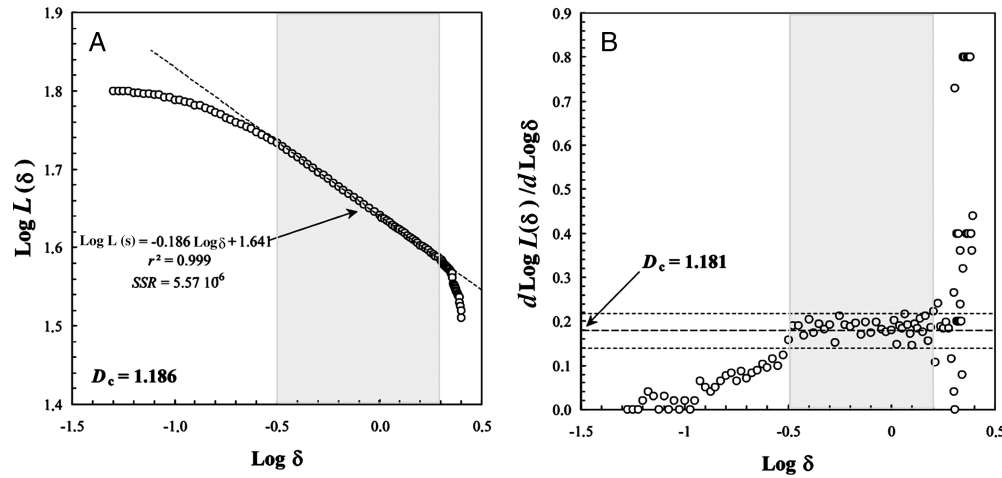


**FIGURE 22.8** Illustration of the  $R^2 - SSR$  (A) and the zero-slope (B) optimization criteria from a 3D swimming pathway of *D. pulex*. In both cases, the shaded areas indicate the scaling ranges. The dotted lines indicate the best regression fit obtained using the  $R^2 - SSR$  criterion (A), and the 5% confidence interval of the flat behavior of  $d \log L(\delta)/d \log \delta$  vs.  $\log \delta$  (dashed line) found using the zero-slope criterion (B).

and

$$d \log N(\lambda) / d \log \lambda = -D_b \quad (22.5)$$

Then if scaling exists, it will manifest as a zero-slope line in plots of both the differentials  $d \log L(\delta)/d \log \delta$  vs.  $\log \delta$ , and  $d \log N(\lambda)/d \log \lambda$  vs.  $\log \lambda$  (Figure 22.8B). Equations 22.4 and 22.5 can thus be rewritten as:

$$d[d \log L(\delta) / d \log \delta] / d \log \delta = 0 \quad (22.6)$$

or equivalently  $[d^2 \log L(\delta) / d^2 \log \delta] = 0$ , and

$$d[d \log N(\lambda) / d \log \lambda] / d \log \lambda = 0 \quad (22.7)$$

or  $[d^2 \log N(\lambda) / d^2 \log \lambda] = 0$ . To ensure the statistical relevance of this procedure, we use a sliding regression window similar to the one described in the  $R^2 - SSR$  procedure. The significance of the differences between the slope of each regression and the expected zero-slope line is directly tested using standard statistical analysis; see Zar (1996). The scaling range will then be defined as the scales that satisfy both Equations 22.6 and 22.7, and the  $R^2 - SSR$  criterion. Finally the intersection of the range of scales exhibiting a zero-slope line with the y-axis provides the compass (see Equation 22.4) and box-counting (see Equation 22.5) dimensions. Hereafter this procedure will be referred to as the “zero-slope” criterion.

Because these procedures may lead to slightly different results in the estimates of the scaling ranges and the related fractal dimensions, we strongly recommend the inclusion in the scaling range of only the scales for which the above two criteria are fully satisfied. In that way, we ensure that the plateau exhibited by the data points in Figure 22.8B is indeed a manifestation of scaling, and not the result of a random nonfractal structure. The implementation of the “ $R^2 - SSR$ ” and “zero-slope” procedures is illustrated using the 3D swimming paths of *D. pulex* (Figure 22.9). It can here be seen that the  $R^2 - SSR$  and the zero-slope criteria lead to slight differences in the estimated scaling ranges (Figure 22.9A, B). In particular, the largest limits of the scaling range are systematically larger ( $p < 0.05$ , Wilcoxon–Mann–Whitney  $U$ -test) when estimated using the zero-slope optimization criterion (Figure 22.9A). The estimates of their lowest limits (Figure 22.9B) cannot be statistically distinguished ( $p > 0.05$ ). These differences did not imply any significant discrepancies between the related compass and box dimensions (Figure 22.9C). Hereafter, these two optimization criteria will nevertheless be systematically used to estimate both compass

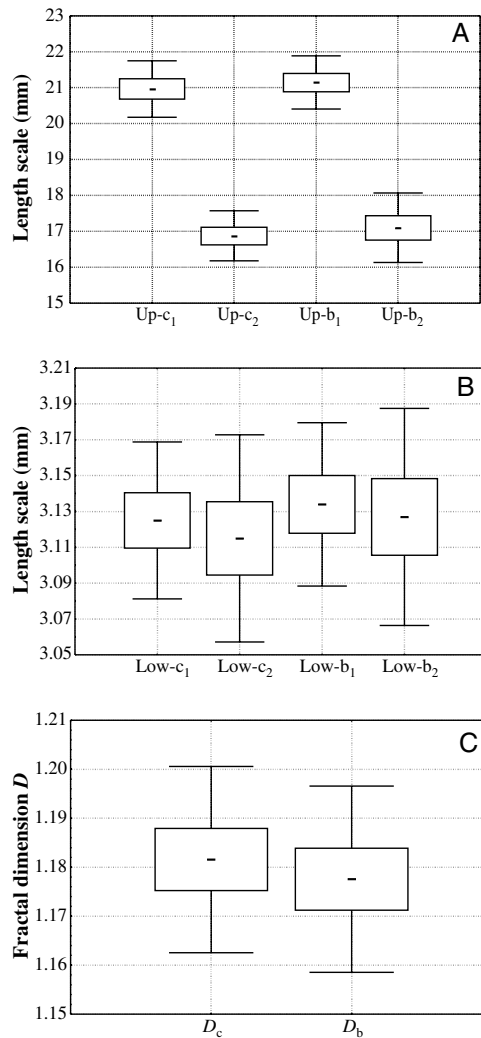


**FIGURE 22.9** Upper (A) and lower (B) limits of the scaling ranges, and related compass and box dimensions (C) obtained from 3D *D. pulex* swimming pathways using the  $R^2 - SSR$  and the zero-slope optimization criteria. The letters “c” and “b” refer to the compass and box-counting methods, and the subscripts “1” and “2” to the  $R^2 - SSR$  and the zero-slope optimization criteria, respectively. The mean  $\bar{x}$  is given within the box (–), the box limits represent  $\bar{x} \pm SE$ , and the outer limits  $\bar{x} \pm SD$ .

and box dimensions. As an example, the absence of such objective criteria in the choice of their scaling range could explain the spurious fractal dimensions ( $D_c < 1$ ) obtained from the 2D behavior of barramundi fish larvae (Dowling et al., 2001, see their figure 1). Moreover, because it appeared from previous arguments that  $D_c \geq 1$  for 2D data, we suggest here that such a result may come from the inclusion of spurious data points in the regression analysis.

### 22.4.3 Robustness of Fractal Dimension Estimating Algorithms

Before addressing ecological interpretations of fractal dimensions estimates, further potential limitations of fractal analysis, intrinsically related to both the compass and the box-counting methods, must be dealt with. It has been shown that (1) the values  $L(\delta) = N\delta$  (i.e., compass method, Equation 22.1) may vary depending on the starting position along the curve (Sugihara and May, 1990), (2) slight reorientations

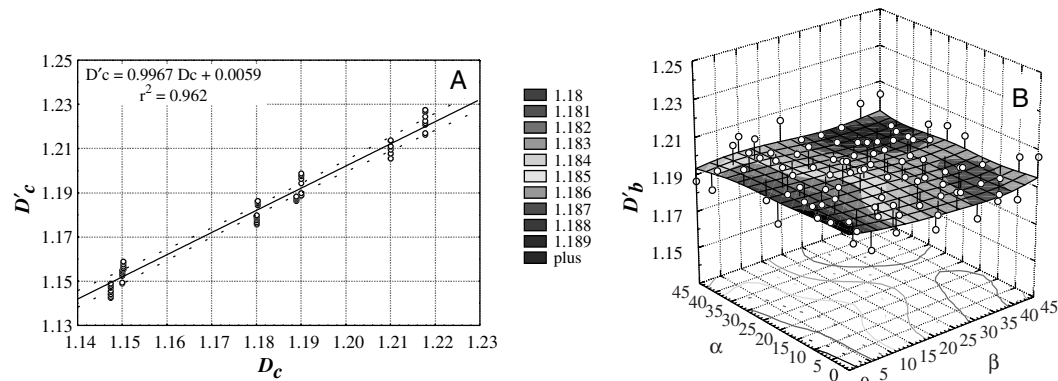


**FIGURE 22.10** Distribution of the compass dimensions  $D'_c$  obtained from ten subpathways with randomly chosen starting positions and the same length within each original 3D swimming pathway of *D. pulex*, and compared to the compass dimensions  $D_c$  obtained from the original nine swimming pathways (A). Box dimensions  $D'_b$  obtained from a 3D swimming path of *D. pulex* using different values of the angles  $\alpha$  and  $\beta$  controlling the position of the 3D box-counting grid in the  $x-y$  and  $x-z$  planes, respectively (B).

of the overlying grid can produce different values of  $N(\lambda)$  (i.e., box-counting method, Equation 22.3; Appleby, 1996), and (3) the values of box dimensions might be positively correlated to a path's length (Erlandson and Kostylev, 1995). Consequently, the behaviors of Equations 22.1 and 22.3 will be biased, as will the subsequent compass and box dimension estimates.

To address the first two issues, distributions of  $D_c$  and  $D_b$  (estimated from 3D swimming paths of *D. pulex*) depending on starting point or grid orientation, respectively, are needed. First, we obtained a distribution of the compass dimension  $D_c$  by repeatedly starting the compass procedure at different, randomly chosen, positions. The resulting compass dimensions  $D'_c$ , estimated from ten random starting positions for each of the nine swimming paths available, do not show significant differences ( $p > 0.05$ ) to the compass dimensions  $D_c$  estimated using the first point of the paths as a starting point for the compass algorithm (Figure 22.10A). Second, we obtained a distribution of the box dimension  $D_b$  from random replicates of the grid placements in the box-counting algorithm. We rotated the initial 3D orthogonal grid in  $5^\circ$  increments from  $\alpha = 0^\circ$  to  $\alpha = 45^\circ$  in the  $x-y$  plane and from  $\beta = 0^\circ$  to  $\beta = 45^\circ$  in the  $x-z$  plane. The resulting box dimension estimates  $D'_b$  fluctuate smoothly around the mean, and did not show any significant tendency related to the variations of  $\alpha$  and  $\beta$  (Figure 22.10B; Friedman test,  $p > 0.05$ ; Siegel and Castellan, 1988).

Finally, the limitation of the box-counting method raised by Erlandson and Kostylev (1995), that the values of box dimensions might be positively correlated to a path's length, has been briefly addressed by comparing the box dimensions obtained from our nine swimming paths of different length (see Table 22.2), and within each data set between ten randomly chosen subsets of decreasing length. The resulting box

**TABLE 22.2**

Duration and Number of Data Points Available from Nine Swimming Paths of *Daphnia pulex* Used to Illustrate Scale-Dependence and Scale-Independence Concepts

Path	N	Duration
1	864	1 min 26 s
2	2413	4 min 01 s
3	1892	3 min 09 s
4	1785	2 min 58 s
5	1733	2 min 53 s
6	2277	3 min 48 s
7	1912	3 min 11 s
8	1460	2 min 25 s
9	1479	2 min 28 s

dimensions  $D_b$ , however, did not show any significant differences between the nine available 3D paths, nor between the ten subsets taken within each available 3D path (covariance analysis,  $F$ -test,  $p > 0.05$ ).

These different results then demonstrate the robustness of the compass and the box-counting algorithms to quantify the structure of *Daphnia*'s paths in three dimensions. Further, one may also note here that the compass dimension  $D_c$  ( $D_c = 1.182 \pm 0.018: \bar{x} \pm SD$ ) and the box dimension  $D_b$  ( $D_b = 1.178 \pm 0.018: \bar{x} \pm SD$ ) estimated in the different ways presented in this section cannot be regarded as being significantly different (Wilcoxon–Mann–Whitney U-test,  $p > 0.05$ ). Although these results suggest that these two techniques can be used interchangeably to characterize *Daphnia*'s paths, we cannot claim their universality. On the contrary, we stress the need to address this question very carefully in the framework of any behavioral studies to ensure the reliability of the results.

### 22.4.4 Two-Dimensional vs. Three-Dimensional Fractal Dimension Estimates

The ability to characterize 3D paths based on 2D projections of these paths is an attractive proposition, as the reduction in complexity of both the data-gathering equipment and the analysis procedures is significant. However, the reliability of conclusions based on such a procedure is not clear. Therefore, we now investigate the consequences of extrapolating fractal dimensions estimated in a 2D framework to three dimensions by first testing the validity of the extrapolation procedures proposed in the literature (Morse et al., 1985; Shorrocks et al., 1991; Gunnarsson, 1992). Second, we investigate the potential for disparity among the fractal dimensions estimated from the three orthogonal 2D projections of a 3D swimming path and, in doing so, demonstrate the necessity of 3D isotropy of a swimming path as a prerequisite for extrapolating 2D fractal information into 3D space.

The philosophy behind the extrapolation of 2D fractal estimates to 3D is as follows: Morse et al. (1985) described a box-counting method for estimating the fractal dimension of vegetation habitats ( $2 \leq D_3 \leq 3$ , where the subscript 3 indicates a fractal object embedded in a 3D space). Consider now the problem of estimating the fractal dimension of a tree branch. In principle, a 3D grid system could be superimposed on the branch and the size of “counting cubes” varied. Such a procedure is impossible to implement in the field, however, at least given present technical limitations. Morse et al. (1985) simplified the problem by obtaining a 2D photographic image of the habitat, the fractal dimension of which was determined using the box-counting method ( $1 \leq D_2 \leq 2$ , where the subscript 2 indicates a fractal object embedded in a 2D space). Following Mandelbrot (1983), they determined heuristic lower ( $D_{3\min} = D_2 + 1$ ) and upper ( $D_{3\max} = 2D_2$ ) limits of the “habitat” fractal dimension under the assumption that the photograph is a randomly placed orthogonal plane. This procedure has subsequently been used to estimate the fractal dimensions of various habitats (e.g., Shorrocks et al., 1991; Gunnarsson, 1992). However, we stress here, on the basis of both simple theoretical and empirical arguments that the use of this procedure to characterize 3D animal paths is at best questionable and, at worst, meaningless.

First, the limits of the extrapolated 3D fractal dimension  $D_3$  are not constant; instead, they increase with increasing values of the 2D fractal dimension  $D_2$ . The disparity between the upper and lower limits range from 4.76 to 31.03% for values of the 2D fractal dimension,  $D_2$ , bounded between 1.10 and 1.90, respectively (Table 22.3). Moreover, for values of  $D_2$  greater than 1.5, the upper limit of the extrapolated fractal dimension  $D_3$  is beyond the maximum space-filling limit  $D_3 = 3$ . Consider now a very complex

**TABLE 22.3**

Standard Procedure to Extrapolate 2D Fractal Dimensions ( $D_2$ ) to 3D Fractal Dimensions ( $D_3$ )

$D_2$	$D_2 + 1$	$2D_2$	IR	$\%D_3 > 3$	
1.10	2.10	2.20	4.76	—	<i>Note:</i> $D_2 + 1$ and $2D_2$ are the lower and the upper limits, respectively, of the extrapolated 3D fractal dimensions; IR is the percentage of increase between the lowest and highest limits of the extrapolated 3D fractal dimensions; and $\%D_3 > 3$ is the percentage of extrapolated 3D fractal dimensions exceeding the space-filling limit $D_3 = d = 3$ .
1.20	2.20	2.40	9.09	—	
1.30	2.30	2.60	13.04	—	
1.40	2.40	2.80	16.67	—	
1.50	2.50	3.00	20.00	—	
1.60	2.60	3.20	23.08	33.33	
1.70	2.70	3.40	25.93	57.14	
1.80	2.80	3.60	28.57	75.00	
1.90	2.90	3.80	31.03	88.89	

swimming path recorded in a 2D space such that  $D_2 \rightarrow 2$ . In this case, the percentage of  $D_3$  values found beyond the space-filling limit,  $D_3 = 3$ , unrealistically tends toward 100% (Table 22.3). This can further be illustrated using the compass dimensions estimated from 2D swimming paths of barramundi fish larvae, which drops from 1.8 prior metamorphosis to 1.1 following metamorphosis (Dowling et al., 2000). Extrapolating the fishes' behavior to three dimensions will lead to reasonable values of  $D_3$  for fish before metamorphosis,  $D_3 \in [2.10 - 2.20]$ . However, for post-metamorphosis fishes, 75% of the  $D_3$  values are beyond the space-filling limit, i.e.,  $D_3 \in [2.80 - 3.60]$ , and cannot therefore be considered legitimate. The validity of this extrapolating procedure is then highly questionable, at least in the framework of behavioral studies. One should nevertheless note here that such extrapolation can only be considered in the case of 2D records of 3D isotropic swimming paths.

Second, investigations of the fractal dimensions estimated from orthogonal 2D projections of 3D swimming paths of *D. pulex* on the  $x - y$ ,  $x - z$ , and  $y - z$  planes illustrate further problems. For example, the fractal dimensions estimated from the  $x - y$ ,  $x - z$  and  $y - z$  projections of the same 3D path ( $D_{2xy}$ ,  $D_{2xz}$  and  $D_{2yz}$ , respectively) are always significantly different (Kruskal-Wallis test,  $p < 0.05$ ). More specifically, the dimensions  $D_{2xz}$  and  $D_{2yz}$  (side views) cannot be distinguished, and are both significantly higher than the dimension  $D_{2xy}$  (top view) (Jonckheere test,  $p > 0.05$  and  $p < 0.05$ , respectively). This suggests that the complexity of the vertical components of the *D. pulex* swimming path is higher than that of its horizontal components, suggesting that the vertical swimming behavior of *D. pulex* is more complex than the horizontal ones. On the other hand, one may note that the average of  $D_{2xy}$ ,  $D_{2yz}$ , and  $D_{2yz}$  is not significantly different from  $D_3$  ( $p > 0.05$ ), due to the intrinsic 3D integrative properties of Equations 22.1 and 22.3. Finally, as expected following the results presented in the previous paragraph, the 3D extrapolations of the 2D fractal dimensions  $D_{2xy}$ ,  $D_{2yz}$  and  $D_{2yz}$  are always significantly higher than the actual 3D fractal dimensions. This has been systematically verified for both compass and box dimensions, estimated in two and three dimensions (Table 22.4). Consequently, it appears that a 2D fractal dimension is not sufficient to characterize 3D swimming behavior if the swimming path is not isotropic.

TABLE 22.4

Fractal Dimensions Obtained Using Box-Counting and Compass Algorithms from 3D Pathways ( $D_3$ ) and Their Three 2D Projections on the  $x - y$ ,  $x - z$ , and  $y - z$  Planes, Shown with the Lowest and Highest Limits of the 3D Dimensions Extrapolated from the 2D Ones

<i>d</i>	<i>D</i>	<i>N</i>	Mean	SD	SE
<i>Box Dimensions D<sub>b</sub></i>					
3	$D_3$	9	1.178	0.055	0.018
2	$D_{2xy}$	9	1.114	0.046	0.015
3 <sub>e</sub>	$D_{2xy} + 1$	9	2.114	1.046	1.015
3 <sub>e</sub>	$2D_{2xy}$	9	2.228	0.092	0.03
2	$D_{2xz}$	9	1.214	0.051	0.017
3 <sub>e</sub>	$D_{xz} + 1$	9	2.214	1.051	1.017
3 <sub>e</sub>	$2D_{2xz}$	9	2.428	0.102	0.034
2	$D_{2yz}$	9	1.199	0.067	0.022
3 <sub>e</sub>	$D_{2yz} + 1$	9	2.199	1.067	1.022
3 <sub>e</sub>	$2D_{2yz}$	9	2.398	0.134	0.044
<i>Compass Dimensions D<sub>c</sub></i>					
3	$D_3$	9	1.182	0.057	0.018
2	$D_{2xy}$	9	1.123	0.048	0.016
3 <sub>e</sub>	$D_{2xy} + 1$	9	2.123	1.048	1.016
3 <sub>e</sub>	$2D_{2xy}$	9	2.246	0.096	0.032
2	$D_{2xz}$	9	1.221	0.052	0.017
3 <sub>e</sub>	$D_{xz} + 1$	9	2.221	1.052	1.017
3 <sub>e</sub>	$2D_{2xz}$	9	2.442	0.104	0.035
2	$D_{2yz}$	9	1.225	0.062	0.020
3 <sub>e</sub>	$D_{2yz} + 1$	9	2.225	1.062	1.020
3 <sub>e</sub>	$2D_{2yz}$	9	2.45	0.124	0.041

Note: *d* is the Euclidean dimension of the considered space;  $D_3$  is the 3D fractal dimension;  $D_{2xy}$ ,  $D_{2xz}$  and  $D_{2yz}$  are the fractal dimensions estimated from the projections of the 3D path on the  $x - y$ ,  $x - z$ , and  $y - z$  planes, respectively; and  $D_{2ij} + 1$  and  $2D_{2ij}$  are the lowest and highest limits of the 3D fractal dimensions extrapolated from the fractal dimensions  $D_{2ij}$  estimated from paths in the  $i - j$  plane.

We also note the seemingly paradoxical result that fractal dimensions estimated from 3D paths are always significantly smaller than 2, the expected lower bound of values for objects embedded in a 3D space. Indeed, following basic fractal theory, an object embedded in a  $d$ -dimensional space should have a fractal dimension bounded between  $d - 1$  and  $d$  (e.g., Mandelbrot, 1983; Schroeder, 1991). In view of this, a linear succession of spaced dust particles will have a dimension bounded between 0 and 1 as they occupy a fraction of the available space greater than a single point (dimension 0), and lower than a line (dimension 1). Similarly, a convoluted curve, a coastline, for example, will occupy a fraction of space between a line (dimension 1) and a surface (dimension 2), while the dimension of a tree will be bounded between 2 (a surface) and 3 (a volume). Now consider again the case of movement paths. The path of an ant foraging on a flat surface occupies a fraction of 2D space. Its dimension is then bounded between 1 (a perfectly linear path) and 2 (a plane-filling path). Similarly, the swimming path of *D. pulex* is obviously embedded in a 3D space, the volume of water (cf. Figure 22.1). However, it does not present a 3D branching structure as does a tree, and each change of direction occurs within a 2D space. Therefore, even in 3D space, a zooplankton swimming path, or the flying path of a foraging bee, will intrinsically remain a convoluted 2D curve. The fractal dimensions of swimming paths are then bounded between a one-dimensional space (i.e., a line,  $D = 1$ ) and a 2D space (i.e., a surface,  $D = 2$ ). The practical consequence of this specific property of swimming paths is to call into question the validity of previous reports of fractal dimensions that fall beyond the  $1 \leq D \leq 2$  limits discussed above for both 2D —  $D_c < 1$  (Dowling et al., 2000) and  $D_c > 2$  (Bascompte and Vilà, 1997) — and 3D ( $D_c > 2$ ; Coughlin et al., 1992) analyses. As suggested above, these discrepancies might result from the lack of some objective procedures to identify the scaling ranges and the subsequent fractal dimensions of movement paths. Considering this, we note that all of the fractal dimensions estimated from *D. pulex* paths were always consistently significantly higher than 1 (linear movement,  $p < 0.01$ ) and lower than 2 (Brownian motion,  $p < 0.01$ ).

## 22.5 Comparing Zooplankton Behavior with the Structure of Their Surrounding Environment

In light of the growing awareness of the scaling nature of marine ecosystems, in both their physical and biological aspects (e.g., Pascual et al., 1995; Seuront and Lagadeuc, 1997, 1998, 2001; Seuront et al., 1996a, b, 1999, 2002; Seuront and Schmitt, 2001; Lovejoy et al., 2001), it is becoming increasingly necessary to find a way to compare the composition of zooplankton swimming behaviors in relation to phytoplankton distributions. In particular, considering the remote sensing ability of zooplankton, their behavior could be strongly influenced by the distribution of their phytoplanktonic prey. Ultimately, knowledge of the precise nature of zooplankton swimming behavior could then be a way to infer the spatial distribution of prey. However, due primarily to technological limitations, it is not yet possible to obtain 3D microscale (i.e., scales smaller than 1 m) distributions of phytoplankton cells *in situ*. On the other hand, it is currently possible to obtain prolonged, simultaneous one-dimensional records (i.e., vertical profiles and time series) of physical (shear, temperature, salinity) and biological (*in vivo* fluorescence, backscatter) parameters at scales below 1 m (see, e.g., Wolk et al., 2001). From such records, one may expect a one-dimensional fractal dimension of phytoplankton distribution  $D = 0.67$  (Seuront and Lagadeuc, 1997; Seuront et al., 2002). In the present study, we found a 3D fractal dimension  $D = 1.18$  (Table 22.4) for *D. pulex* swimming behavior. Unfortunately, a direct comparison of these two dimensions is not possible because they characterize two processes embedded in different dimensions (Roy et al., 1987; Huang and Turcotte, 1989). We nevertheless propose here a more fundamental framework, the fractal codimension, which makes possible comparisons of the structure of processes embedded in different  $d$ -dimensional spaces. The fractal codimension  $c$  has been defined as (Seuront, 1998; Seuront et al., 1999):

$$c = d - D \quad (22.8)$$

where  $d$  is the Euclidean dimension of the embedding space and  $D$  the fractal dimension of a given process. The fractal codimension, then, measures the fraction of the dimensional space occupied by the process of

interest, and is bounded between  $c = 0$  and  $c = 1$  for “standard” processes characterized by a fractal dimension  $D$  such as  $d - 1 \leq D \leq d$ . Because the fractal dimension  $D$  of swimming paths is intrinsically bounded between  $1 \leq D \leq 2$ , whatever the value of the embedded dimension  $d$ , for more generality we can consider a fractal codimension bounded between  $c = 0$  and  $c = d$ . However, in such a framework, comparisons of codimensions estimated from processes embedded in different  $d$ -dimensional space are unfeasible without *a priori* knowledge of the embedding dimension  $d$ . The fractal codimension subsequently provides only a relative measure of sparseness. We therefore introduce here the “path codimension”  $c'$ :

$$c' = c/d \quad (22.9)$$

as an absolute measure of sparseness.  $c'$  is bounded between  $c' = 0$  for space-filling processes, and  $c' = 1$  for processes so sparse that their fractal dimension is nil, whatever the values of the original embedding dimensions  $d$  may be. Returning to the example above, the path codimensions of phytoplankton distribution and *D. pulex* behavior are  $c' = 0.33$  and  $c' = 0.61$ , respectively. Thus, the swimming behavior of *D. pulex* appears to be less complex, or less space filling, than the distribution of its phytoplankton fodder. In particular, this result fully agrees with studies demonstrating the differences in motility between predators and prey (e.g., Tiselius et al., 1993, 1997; Seuront and Lagadeuc, 2001). In general, the path codimension provides a method of comparing the complexity of two interrelated processes, each of which may be embedded in a different dimensional space.

## 22.6 Conclusion

In this chapter, we have discussed the basic concepts and methods related to the fractal framework, and subsequently attempted to address the major issues related to the applicability of fractal analysis in behavioral ecology. We have tried to clarify some problematic aspects of behavioral fractal analysis, and we propose that the following recommendations are fundamental requirements for improving the robustness of fractal analyses, which in turn ensures that their interpretation will be meaningful:

1. The key component of fractal analysis is not that the fractal dimension  $D$  is a scale-independent parameter. Alternatively, we argue that the potential scale dependence of fractal dimensions over finite ranges of scales may contain more information, both in terms of driving processes and sampling limitation, than its scale dependence over a hypothetical infinite range of scales. To ensure the relevance of fractal analysis, the key issue is related to a proper estimation of the scaling range.
2. Considering the lack of objective criteria for testing the existence of scaling properties in animal paths, we present two complementary, easy to implement, robust, and statistically sound procedures to identify scaling properties and estimate fractal dimensions. More generally, we strongly recommend use of a combination of two optimization criteria to identify a scaling range.
3. We address the major objections proposed against the use of fractal analyses in ecology and demonstrate, using a series of simple testing procedures, their robustness in estimating the fractal dimensions of animal paths.
4. In an investigation of the 2D and 3D fractal properties of paths, we emphasize some intrinsic geometric properties of movement paths, and stress the need to ensure their 3D isotropy. This can be done only by comparing the fractal dimension of the three 2D projections of a 3D path.
5. We introduce a new metric, the “path codimension,” which can be used to compare the absolute sparseness of related processes that are embedded in different  $d$ -dimensional spaces.

However, the main purpose of the chapter has been to confirm the ability of fractal methods to provide both qualitative and quantitative characterizations of animal paths in 2D and 3D environments. Subsequently, considering the ubiquitous geometrical nature of animal movements, we believe that our approach can be generalized to the behavior of all moving organisms. However, we emphasize that the conclusions drawn here, essentially on the robustness of fractal dimension estimates, should

not be generalized to other fractal objects such as the structure of landscape heterogeneity or vegetation branching processes without preliminary, careful investigations of the properties of the algorithms involved.

We have illustrated all the concepts discussed above by applying this fractal framework to the study of 3D swimming behavior of the water flea *Daphnia pulex*. The subsequent results, while only at their preliminary stage, nevertheless have generated several salient implications for our understanding of structures and functions in marine ecosystems:

1. Because individual swimming behavior is the underlying mechanism generating population-level behaviors such as horizontal and vertical migration, the horizontal–vertical disparity in *D. pulex* swimming behavior may reflect an adaptive reminiscence of diel vertical migration as a predator avoidance strategy (Loose, 1992; Loose et al., 1992). The difference in fractal behavior identified in the horizontal and the vertical planes may also be suggested as a basis to investigate the predation risk associated with differential swimming behavior related to mating, feeding, or predator avoidance strategies. Fractal evaluation of 2D coordinates of 3D swimming paths is thus particularly useful in this context. Depending on the relative velocities of predator and prey, a swimming behavior characterized by a high fractal dimension may imply a high encounter probability with predators, relative to a more linear swimming path. In addition, a high fractal dimension may also imply a higher encounter probability with prey, depending on the foraging strategy employed (e.g., an ambush or saltatory search predator will have a higher fractal dimension swimming path with an increased level of prey).
2. Individual behavior affects the outcome of predator–prey interactions, especially in the pelagic environment, where prey movement is important both as a cue to predators (Brewer and Coughlin, 1995) and a determinant of encounter rate (Gerritsen and Strickler, 1977). Moreover, the distribution of prey organisms is very important for predators, as recently investigated numerically (Seuront, 2001; Seuront et al., 2001), because food availability changes depending on the fractal dimension. Low fractal dimensions indicate a smooth and predictable distribution of particles gathered in small numbers of patches, whereas high fractal dimensions indicate rough, fragmented, space-filling, and less predictable distributions. Therefore, when a predator can remotely detect its surroundings, prey distributions with low dimension should be more efficient. In contrast, when a predator has no remote detection ability, prey distributions with high dimension should be preferable, because available food quantity or encounter rate becomes proportional to the searched volume as fractal dimension increases. The comparison of the fractal nature of plankton swimming behavior and plankton distributions will then increase our understanding of zooplankton trophodynamics. For example, Johnson et al. (1992b) discussed the interaction between animal movement characteristics and the patch-boundary features in a “microlandscape.” They argued that such interactions have important spatial consequences on gene flow, population dynamics, and other ecological processes in the community (see also Wiens et al., 1995). In the ocean, which is increasingly regarded as a “seascape” considering the growing awareness of the heterogeneous nature of microscale processes, behavioral studies would be of prime interest to improve our understanding of the functioning of marine ecosystems from a bottom-up view (Seuront, 2001; Seuront et al., 2001). Although such information is not yet available, we believe that the quickly advancing technology (e.g., Wolk et al., 2002; Franks and Jaffe, 2001) will ensure the achievement of this goal in the near future.
3. Individual feeding rate may be linked to swimming behavior; in most zooplankton, some of the same appendages are used for both behaviors. Considering the actual evidence for prey switching behavior (e.g., Kiørboe et al., 1996; Caparroy et al., 1998), fractal analysis may be suggested as a diagnostic framework to access the kind of prey zooplankton preferentially feed on in a plurispecific prey assemblage. On the other hand, swimming behavior differs among species (Tiselius and Jonsson, 1990) and among development stages within a species (van Duren and Videler, 1995). Attempts at modeling the grazing pressure resulting from both mono- or plurispecific zooplankton assemblages could then benefit from an incorporation of potential differences in swimming path complexity. For example, in a comparison of path tortuosity in

three species of grasshopper, With (1994a) found that the path fractal dimension of the largest species was smaller than those of the two smaller species. She suggested that this reflects the fact that smaller species interact with the habitat at a finer scale of resolution than do larger species. In a second study, With (1994b) found differences in the ways that gomphocerine grasshopper nymphs and adults interacted with the microlandscape. Similarly, the knowledge of the precise nature of the swimming behavior has been suggested as a way to infer the spatial distribution of foragers (Turchin, 1991; Seuront and Lagadeuc, 2001).

4. Toxic chemicals (whether natural, such as cyanobacterial toxins, or anthropogenic, such as pesticides) can have indirect effects on the entire pelagic community via effects on individual swimming behavior (Dodson et al., 1995). The demonstrated sensitivity of fractal analysis may then provide an efficient framework to use the swimming behavior of *Daphnia*, or some other zooplankton organisms, as a “living toxicometer.”
5. Finally, we stress here that an important consequence of the fractal nature of zooplankton swimming behavior, illustrated here using 3D *D. pulex* paths, is its deviation from Brownian motion. Fractional Brownian motion models (Mandelbrot, 1983; Schroeder, 1991) have been suggested to characterize the movement of organisms (Frontier, 1987). However, Wiens and Milne (1989), examining beetle movements in natural fractal landscapes, found that observed beetle movements deviated from the modeled (fractional Brownian) ones. A follow-up study by Johnson et al. (1992a) found that beetle movements reflect a combination of ordinary (random) and anomalous diffusions. The latter may simply reflect intrinsic departures from randomness, or result from barrier avoidance and utilization of corridors in natural landscapes. An extensive discussion of the anomalous diffusion of a copepod in a heterogeneous environment can be found elsewhere (Marguerit et al., 1998; Schmitt and Seuront, 2001). Future modeling attempts of zooplankton swimming behavior may have to take into account the nonrandomness (i.e., fractal) of organisms’ movements, and the persistence of the direction of travel (cf. Figure 22.3A), as recently suggested by Wu et al. (2000) and Schmitt and Seuront (2001).

This chapter has highlighted areas concerning the valid applications of fractal analysis so that it can be used to faithfully represent the ecological effect of plankton behavior as is found in aquatic systems. This precision should be a fundamental requirement for integrated behavioral components in plankton models (Seuront, 2001; Seuront et al., 2001; Ginot et al., 2002; Yamazaki and Kamykowski, Chapter 35, this volume; Souissi and Bernard, Chapter 23, this volume) in order for their results to be ecologically relevant. Whatever the case, the understanding of zooplankton ecology from the behavioral bottom-up approach is still in its infancy.

---

## References

- Abraham, E.R., 2001. The fractal branching of an arborescent sponge. *Mar. Biol.*, 138, 503–510.
- Appleby, S., 1996. Multifractal characterization of the distribution pattern of the human population. *Geogr. Anal.*, 28, 147–160.
- Bascompte, J. and Vilà, C., 1997. Fractals and search paths in mammals. *Land. Ecol.*, 12, 213–221.
- Batschelet, E., 1981. *Circular Statistics in Biology*. Academic Press, New York.
- Bell, W.J., 1991. *Searching Behavior, the Behavioral Ecology of Finding Resources*. Chapman & Hall, New York.
- Bergman, C.M., Schaefer, J.A., and Luttich, S.N., 2000. Caribou movement as a correlated random walk. *Oecologia*, 123, 364–374.
- Boinski, S. and Garber, P.A., 2000. *On the Move. How and Why Animals Travel in Groups*. University of Chicago Press, Chicago.
- Bradbury, R.H. and Reichelt, R.E., 1983. Fractal dimension of a coral reef at ecological scales. *Mar. Ecol. Prog. Ser.*, 10, 169–171.
- Bradbury, R.H., Reichelt, R.E., and Green, D.G., 1984. Fractals in ecology: methods and interpretation. *Mar. Ecol. Prog. Ser.*, 14, 295–296.

- Brewer, M.C., 1996. *Daphnia* Swimming Behavior and Its Role in Predator–Prey Interactions. Ph.D. thesis, University of Wisconsin–Milwaukee, 155 pp.
- Brewer, M.C., 1998. Mating behaviours of *Daphnia pulicaria*, a cyclic parthenogen: comparisons with copepods. *Philos. Trans. R. Soc. Lond. B*, 353, 805–815.
- Brewer, M.C. and Coughlin, J.N., 1995. Virtual plankton: a novel approach to the investigation of aquatic predator–prey interactions. *Mar. Freshw. Behav.*, 26, 91–100.
- Buchanan, C., Goldberg, B., and McCartney, R., 1982. A laboratory method for studying zooplankton swimming behaviors. *Hydrobiologia*, 94, 77–89.
- Bundy, M.H., Gross, T.F., Coughlin, D.J., and Strickler, J.R., 1993. Quantifying copepod searching efficiency using swimming pattern and perceptive ability. *Bull. Mar. Sci.*, 53, 15–28.
- Burlando, B., 1990. The fractal dimension of taxonomic systems. *J. Theor. Biol.*, 146, 99–114.
- Burlando, B., 1993. The fractal dimension geometry of evolution. *J. Theor. Biol.*, 163, 161–172.
- Buskey, E.J., 1984. Swimming pattern as an indicator of the roles of copepod sensory systems in the recognition of food. *Mar. Biol.*, 79, 165–175.
- Buskey, E.J., 1997. Behavioral components of feeding selectivity of the heterotrophic dinoflagellate *Prorocentrum pellucidum*. *Mar. Ecol. Prog. Ser.*, 153, 776–789.
- Buskey, E.J. and Stoecker, D.K., 1988. Locomotory patterns of the planktonic ciliate *Favella* sp.: adaptations for remaining within food patches. *Bull. Mar. Sci.*, 43, 783–796.
- Buskey, E.J., Mills, L., and Swift, E., 1983. The effects of dinoflagellate bioluminescence on the swimming behavior of a marine copepod. *Limnol. Oceanogr.*, 28, 575–579.
- Buskey, E.J., Coulter, C., and Strom, S., 1993. Locomotory patterns of microzooplankton: potential effects on food selectivity of larval fish. *Bull. Mar. Sci.*, 53, 29–43.
- Buskey, E.J., Peterson, J.O., and Ambler, J.W., 1996. The swarming behavior of the copepod *Dioithona oculata*: *in situ* and laboratory studies. *Limnol. Oceanogr.*, 41, 513–521.
- Caparroy, P., Pérez, M.T., and Carlotti, F., 1998. Feeding behaviour of *Centropages typicus* in calm and turbulent conditions. *Mar. Ecol. Prog. Ser.*, 168, 109–118.
- Charoy, C.P., Janssen, C.R., Persoone, G., and Clément, P., 1995. The swimming behaviour of *Brachiomus calyciflorus* (rotifer) under toxic stress. I. The use of automated trajectometry for determining sub-lethal effects of chemicals. *Aquat. Toxicol.*, 32, 271–282.
- Cody, M.L., 1971. Finch flocks in the Mohave desert. *Theor. Popul. Biol.*, 163, 161–172.
- Costello, J.H., Strickler, J.R., Marrasé, C., Trager, G., Zeller, R., and Freise, A.J., 1990. Grazing in a turbulent environment: behavioral response of a calanoid copepod, *Centropages hamatus*. *Proc. Natl. Acad. Sci. U.S.A.*, 87, 1648–1652.
- Coughlin, D.J., Strickler, J.R., and Sanderson, B., 1992. Swimming and search behaviour in clownfish, *Amphiprion perideraion*, larvae. *Anim. Behav.*, 44, 427–440.
- Cowles, T.J., Desiderio, R.A., and Carr, M.E., 1998. Small-scale planktonic structure: persistence and trophic consequences. *Oceanography*, 11, 4–9.
- Crist, T.O., Guertin, D.S., Wiens, J.A., and Milne, B.T., 1992. Animal movement in heterogeneous landscapes: an experiment with *Elodes* beetles in shortgrass prairie. *Functional Ecol.*, 6, 536–544.
- Dodson, S. and Ramcharan, C., 1991. Size specific swimming behavior of *Daphnia pulex*. *J. Plankton Res.*, 13, 1367–1379.
- Dodson, S.I., Hanazato, T., and Gorski, P.R., 1995. Behavioral responses of *Daphnia pulex* exposed to carbaryl and *Chaoborus* kairomone. *Environ. Toxicol. Chem.*, 14, 43–50.
- Dodson, S.I., Ryan, S., Tollrian, R., and Lampert, W., 1997. Individual swimming behavior of *Daphnia*: effects of food, light and container size in four clones. *J. Plankton Res.*, 19, 1537–1552.
- Dowling, N.A., Hall, S.J., and Mitchell, J.G., 2001. Foraging kinematics of barramundi during early stages of development. *J. Fish Biol.*, 57, 337–353.
- Erlandson, J. and Kostylev, V., 1995. Trail following, speed and fractal dimension of movement in a marine prosobranch, *Littorina littorea*, during a mating and a nonmating season. *Mar. Biol.*, 122, 87–94.
- Fielding, A., 1992. Applications of fractal geometry to biology. *Comput. Appl. Biosci.*, 8, 359–366.
- Fisher, R., Bellwood, D.R., and Job, S.D., 2000. Development of swimming abilities in reef fish larvae. *Mar. Ecol. Prog. Ser.*, 202, 163–173.
- Franks, P.J.S. and Jaffe, J.S., 2001. Microscale distributions of phytoplankton: initial results from a two-dimensional imaging fluorometer, OSST. *Mar. Ecol. Prog. Ser.*, 220, 59–72.

- Frontier, S., 1985. Diversity and structure in aquatic ecosystems. *Oceanogr. Mar. Biol. Annu. Rev.*, 23, 253–312.
- Frontier, S., 1987. Applications of fractal theory to ecology, in Legendre, P. and Legendre, L., Eds., *Developments in Numerical Ecology*. Springer, Berlin, 335–378.
- Frontier, S., 1994. Species diversity as a fractal property of biomass, in Novak, M.M., Ed., *Fractals in the Natural and Applied Sciences*. Elsevier, New York, 119–127.
- Gardner, R.H., O'Neill, R.V., Turner, M.G., and Dale, V.H., 1989. Quantifying scale-dependent effects of animal movement with simple percolation models. *Land. Ecol.*, 3, 217–227.
- Gaustestad, A.O. and Myserud, I., 1993. Physical and biological mechanisms in animal movement processes. *J. Appl. Ecol.*, 30, 523–535.
- Gee, J.M. and Warwick, R.M., 1994a. Body-size distribution in a marine metazoan community and the fractal dimensions of macroalgae. *J. Exp. Mar. Biol. Ecol.*, 178, 247–259.
- Gee, J.M. and Warwick, R.M., 1994b. Metazoan community structure in relation to the fractal dimensions of marine macroalgae. *Mar. Ecol. Prog. Ser.*, 103, 141–150.
- Gerritsen, J. and Strickler, J.R., 1977. Encounter probabilities and community structure in zooplankton: a mathematical model. *J. Fish. Res. Board Can.*, 34, 73–82.
- Ginot, V., Le Page, C., and Souissi, S., 2002. A multi-agent architecture to enhance end-user individual based modelling. *Ecol. Model.* 157, 23–41.
- Goldberger, A.L., Bhargava, V., Wesr, B.J., and Mandell, A.J., 1985. On a mechanism of cardiac electrical stability. The fractal hypothesis. *Biophys. J.*, 48, 525–528.
- Gries, T., Jöhnk, K., Fields, D., and Strickler, J.R., 1999. Size and structure of “footprints” produced by *Daphnia*: impact of animal size and density gradients. *J. Plankton Res.*, 21, 509–523.
- Gunnarsson, B., 1992. Fractal dimension of plants and body size distribution in spiders. *Funct. Ecol.*, 6, 636–641.
- Hamilton, S.K., Melack, J.M., Goodchild, M.F., and Lewis, W.M., 1992. Estimation of the fractal dimension of terrain from lake size distributions, in Carling, P.A. and Petts, G.E., Eds., *Lowland Floodplain Rivers: Geomorphological Perspectives*. John Wiley & Sons, New York, 145–163.
- Hastings, H.M. and Sugihara, G., 1993. *Fractals. A User's Guide for the Natural Sciences*. Oxford University Press, Oxford.
- Huang, J. and Turcotte, D.L., 1989. Fractal mapping of digitized images: application to the topography of Arizona and comparisons with synthetic images. *J. Geophys. Res.*, 94, 7491–7495.
- Hwang, J.S. and Strickler, J.R., 1994. Effects of periodic turbulent events upon escape responses of a calanoid copepod, *Centropages hamatus*. *Bull. Plankton Soc. Jpn.*, 41, 117–130.
- Hwang, J.S., Costello, J.H., and Strickler, J.R., 1994. Copepod grazing in turbulent flow: elevated foraging behavior and habituation to escape responses. *J. Plankton Res.*, 16, 421–431.
- Johnson, A.R. and Milne, B.T., 1992. Diffusion in fractal landscapes: simulations and experimental studies of tenebrionid beetle movements. *Ecology*, 73, 1968–1983.
- Johnson, A.R., Milne, B.T., and Wiens, J.A., 1992a. Diffusion in fractal landscapes: simulations and experimental studies of tenebrionid beetle movements. *Ecology*, 73, 1968–1983.
- Johnson, A.R., Wiens, J.A., Milne, B.T., and Crist, T.O., 1992b. Animal movements and population dynamics in heterogeneous landscapes. *Land. Ecol.*, 7, 63–75.
- Jonsson, P.R. and Johansson, M., 1997. Swimming behaviour, patch exploitation and dispersal capacity of a marine benthic ciliate in flume flow. *J. Exp. Mar. Biol. Ecol.*, 215, 135–153.
- Kareiva, P.M. and Shigesada, N., 1983. Analyzing insect movement as a correlated random walk. *Oecologia*, 56, 234–238.
- Keiyu, A.Y., Yamazaki, H., and Strickler, R., 1994. A new modelling approach for zooplankton behaviour. *Deep-Sea Res. I*, 41, 171–184.
- Kenkel, N.C. and Walker, D.J., 1993. Fractals and ecology. *Abstr. Bot.*, 17, 53–70.
- Kjørboe, T., Saiz, E., and Viitasalo, M., 1996. Prey switching behaviour in the planktonic copepod *Acartia tonsa*. *Mar. Ecol. Prog. Ser.*, 143, 65–75.
- Lampert, W., 1987. Feeding and nutrition in *Daphnia*, in Peters, R.H. and De Bernardi, R., Eds., *Daphnia. Mem. Del. Inst. Ital. Di Idrobiol.*, 143–192.
- Larson, P. and Kleiven, O.T., 1996. Food search and swimming speed in *Daphnia*, in Lenz, P.H., Hartline, D.K., Purcell, J.E., and Macmillan, D.L., Eds., *Zooplankton: Sensory Ecology and Physiology*. Gordon & Breach, Amsterdam, 375–387.

- Leising, A.W., 2001. Copepod foraging in patchy habitats and thin layers using a 2-D individual based model. *Mar. Ecol. Prog. Ser.*, 216, 167–179.
- Leising, A.W. and Franks, P.J.S., 2000. Copepod vertical distribution within a spatially variable food source: a simple foraging-strategy model. *J. Plankton Res.*, 22, 999–1024.
- Li, X., Passow, U., and Logan, B.E., 1998. Fractal dimension of small (15–200  $\mu\text{m}$ ) particles in Eastern Pacific coastal waters. *Deep-Sea Res. I*, 45, 115–132.
- Loehle, C., 1983. The fractal dimension and ecology. *Specul. Sci. Tech.*, 6, 131–142.
- Loehle, C., 1990. Home range: a fractal approach. *Land. Ecol.*, 5, 39–52.
- Longley, P.A. and Batty, M., 1989. On the fractal measurement of geographical boundaries. *Geogr. Anal.*, 21, 47–67.
- Loose, C.J., 1992. *Daphnia* diel vertical migration behavior: response to vertebrate predator abundance. *Arch. Hydrobiol. Beih.*, 39, 29–36.
- Loose, C.J., Von Elert, E., and Dawidowicz, P., 1992. Chemically-induced diel vertical migration in *Daphnia*: a new bioassay for kairomones exuded by fish. *Arch. Hydrobiol.*, 126, 329–337.
- Lovejoy, S., Currie, W.J.S., Tessier, Y., Claereboudt, M.R., Bourget, E., Roff, J.C., and Schertzer, D., 2001. Universal multifractals and ocean patchiness: phytoplankton, physical fields and coastal heterogeneity. *J. Plankton Res.*, 23, 117–141.
- Mach, J., Mas, F., and Saguès, F., 1994. Laplacian multifractality of the growth probability distribution in electrodeposition. *Europhys. Lett.*, 25, 217–276.
- Maly, E.J., van Leeuwen, H.C., and Blais, J., 1994. Some aspects of size and swimming behavior in two species of *Diaptomus* (Copepoda: Calanoida). *Verh. Int. Verein. Limnol.*, 25, 2432–2435.
- Mandelbrot, B., 1977. *Fractals. Form, Chance and Dimension*. W.H. Freeman, London.
- Mandelbrot, B., 1983. *The Fractal Geometry of Nature*. W.H. Freeman, New York.
- Marguerit, C., Schertzer, D., Schmitt, F., and Lovejoy, S., 1998. Copepod diffusion within multifractal phytoplankton fields. *J. Mar. Syst.*, 16, 69–83.
- Marrasé, C., Coastello, J.H., Granata, T., and Strickler, J.R., 1990. Grazing in a turbulent environment: behavioral response of a calanoid copepod, *Centropages hamatus*. *Proc. Natl. Acad. Sci. U.S.A.*, 87, 1652–1657.
- McCulloch, C.E. and Cain, M.L., 1989. Analyzing discrete movement data as a correlated random walk. *Ecology*, 70, 383–388.
- Mitchell, J.G. and Furhman, J.A., 1989. Centimeter scale vertical heterogeneity and chlorophyll *a*. *Mar. Ecol. Prog. Ser.*, 54, 141–148.
- Morse, D.H., 1980. *Behavioral Mechanisms in Ecology*. Harvard University Press, Cambridge, MA.
- Morse, D.R., Lawton, J.H., Dodson, M.M., and Williamson, M.H., 1985. Fractal dimension of vegetation and the distribution of arthropod body lengths. *Nature*, 314, 731–733.
- O'Keefe, T.C., Brewer, M.C., and Dodson, S.I., 1998. Swimming behavior of *Daphnia*: its role in determining predation risk. *J. Plankton Res.*, 20, 973–984.
- Paffenhöffer, G.A., Strickler, J.R., Lewis, K.D., and Richman, S., 1996. Motion behavior of nauplii and early copepodid stages of marine planktonic copepods. *J. Plankton Res.*, 18, 1699–1715.
- Pascual, M., Ascioti, F.A., and Caswell, H., 1995. Intermittency in the plankton: a multifractal analysis of zooplankton biomass variability. *J. Plankton Res.*, 17, 1209–1232.
- Peitgen, H.O., Jürgensand, H., and Saupe, D., 1992. *Fractals for the Classroom*. Springer, New York.
- Pietronero, L. and Labini, F.S., 2000. Fractal universe. *Physica A*, 280, 125–130.
- Porter, K.G., Gerritsen, J., and Orcutt, J.D., 1982. The effect of food concentration on swimming patterns, feeding behavior, ingestion, assimilation and respiration in *Daphnia*. *Limnol. Oceanogr.*, 27, 935–949.
- Price, H.J., 1989. Feeding mechanisms of krill in response to algal patches: a mesocosm study. *Limnol. Oceanogr.*, 34, 649–659.
- Provata, A. and Almirantis, Y., 2000. Fractal cantor patterns in the sequence structure of DNA. *Fractals*, 8, 15–27.
- Pyke, G.H., 1981. Optimal foraging in hummingbirds: rule of movement between inflorescences. *Anim. Behav.*, 29, 882–896.
- Pyke, J.H., 1984. Optimal foraging theory: a critical review. *Annu. Rev. Ecol. Syst.*, 15, 523–575.
- Ramcharan, C.W. and Sprules, W.G., 1991. Predator-induced behavioral defense and its ecological consequences for two calanoid copepods. *Oecologia*, 86, 276–286.
- Ringelberg, J., 1964. The positively photoactive reaction of *Daphnia magna* Strauss: a contribution to the understanding of diurnal vertical migration. *Neth. J. Sea Res.*, 2, 319–406.

- Roy, A.G., Gravel, G., and Gauthier, C., 1987. Measuring the dimension of surfaces: a review and appraisal of different methods, in *Proceedings, 8th International Symposium on Computer-Assisted Cartography (Auto-Carto 8)*, Baltimore, MD, 68–77.
- Saiz, E., 1994. Observations of the free-swimming behavior of *Acartia tonsa*: effects of food concentration and turbulent water motion. *Limnol. Oceanogr.*, 39, 1566–1578.
- Saiz, E. and Alcaraz, M., 1992. Free-swimming behaviour of *Acartia clausi* (Copepoda: Calanoida) under turbulence water movement. *Mar. Ecol. Prog. Ser.*, 80, 229–236.
- Schmitt, F. and Seuront, L., 2001. Multifractal random walk in copepod behavior. *Physica A*, 301, 375–396.
- Schmitt, F. and Seuront, L., 2002. Multifractal anomalous diffusion in swimming behavior of marine organisms, in Pomeau, Y. and Ribotta, A., Eds., *Proc. 5th Rencontre du Non-linéaire*, Paris, Institut Poincaré. Non-linéaire publications, Paris, 237–242.
- Schroeder, M., 1991. *Fractals, Chaos, Power Laws*. W.H. Freeman, New York.
- Seuront, L., 1998. Fractals and multifractals: new tools to characterize space–time heterogeneity in marine ecology. *Océanis*, 24, 123–158.
- Seuront, L., 2001. Microscale processes in the ocean: why are they so important for ecosystem functioning? *La Mer*, 39, 1–8.
- Seuront, L. and Lagadeuc, Y., 1997. Characterisation of space–time variability in stratified and mixed coastal waters (Baie des Chaleurs, Quebec, Canada): application of fractal theory. *Mar. Ecol. Prog. Ser.*, 159, 81–95.
- Seuront, L. and Lagadeuc, Y., 1998. Spatio-temporal structure of tidally mixed coastal waters: variability and heterogeneity. *J. Plankton Res.*, 20, 1387–1401.
- Seuront, L. and Lagadeuc, Y., 2001. Multiscale patchiness of the calanoid copepod *Temora longicornis* in a turbulent coastal sea. *J. Plankton Res.*, 23, 1137–1145.
- Seuront, L. and Schmitt, F., 2001. Describing intermittent processes in the ocean: univariate and bivariate multiscaling procedures, in Müller, P. and Garrett, C., Eds., *Stirring and Mixing in a Stratified Ocean*. SOEST, University of Hawaii, 12, 131–144.
- Seuront, L., Schmitt, F., Schertzer, D., Lagadeuc, Y., and Lovejoy, S., 1996a. Multifractal intermittency of Eulerian and Lagrangian turbulence of ocean temperature and plankton fields. *Nonlinear Proc. Geophys.*, 3, 236–246.
- Seuront, L., Schmitt, F., Lagadeuc, Y., Schertzer, D., Lovejoy, S., and Frontier, S., 1996b. Multifractal analysis of phytoplankton biomass and temperature in the ocean. *Geophys. Res. Lett.*, 23, 3591–3594.
- Seuront, L., Schmitt, F., Lagadeuc, Y., Schertzer, D., and Lovejoy, S., 1999. Universal multifractal analysis as a tool to characterize multiscale intermittent patterns: example of phytoplankton distribution in turbulent coastal waters. *J. Plankton Res.*, 21, 877–922.
- Seuront, L., Schmitt, F., and Lagadeuc, Y., 2001. Turbulence intermittency, phytoplankton patchiness and encounter rates in plankton: where do we go from here? *Deep-Sea Res. I*, 48, 1199–1215.
- Seuront, L., Gentilhomme, V., and Lagadeuc, Y., 2002. Small-scale nutrient patches in tidally mixed coastal waters. *Mar. Ecol. Prog. Ser.* 232, 29–44.
- Shlesinger, M.F. and West, B.J., 1991. Complex fractal dimension of the bronchial tree. *Phys. Rev. Lett.*, 67, 2106–2108.
- Shorrocks, B., Marsters, J., Ward, I., and Evennett, P.J., 1991. The fractal dimension of lichens and the distribution of arthropod body lengths. *Funct. Ecol.*, 5, 457–460.
- Siegel, S. and Castellan, N.J., 1988. *Nonparametric Statistics*. McGraw-Hill, New York.
- Siniff, D.B. and Janssen, C.R., 1969. A simulation model of animal movement patterns. *Adv. Ecol. Res.*, 6, 185–219.
- Squires, K.D. and Yamazaki, H., 1995. Preferential concentration of marine particle in isotropic turbulence. *Deep-Sea Res.*, 42, 1989–2004.
- Stevens, D.W. and Krebs, J.R., 1986. *Foraging Theory*. Princeton University Press, Princeton, NJ.
- Strickler, J.R., 1970. Über das Schwimmverhalten von Cyclopoiden bei Verminderungen des Bestrahlungsstarke. *Schweiz. Z. Hydrobiol.*, 32, 150–180.
- Strickler, J.R., 1985. Feeding currents in calanoid copepods: two new hypotheses. *Symp. Soc. Exp. Biol.*, 39, 459–485.
- Strickler, J.R., 1992. Calanoid copepods, feeding currents, and the role of gravity. *Science*, 218, 158–160.
- Strickler, J.R., 1998. Observing free-swimming copepods mating. *Philos. Trans. R. Soc. Lond. B*, 353, 671–680.
- Suchman, C.L., 2000. Escape behavior of *Acartia hudsonica* copepods during interactions with scyphomedusae. *J. Plankton Res.*, 22, 2307–2323.

- Sugihara, G. and May, R.M., 1990. Applications of fractals in ecology. *TREE*, 5, 79–86.
- Tang, S., Ma, Y., and Sebastine, I.M., 2001. The fractal nature of *Escherichia coli* biological flocs. *Colloids Surf. B Interfaces*, 20, 211–218.
- Tarafdar, S., Franz, A., Schulzky, C., and Hoffman, K.H., 2001. Modelling porous structures by repeated Sierpinski carpets. *Physica A*, 292, 1–8.
- Tiselius, P., 1992. Behavior of *Acartia tonsa* in patchy food environments. *Limnol. Oceanogr.*, 37, 1640–1651.
- Tiselius, P. and Jonsson, P.R., 1990. Foraging behaviour of six calanoid copepods: observations and hydrodynamic analysis. *Mar. Ecol. Prog. Ser.*, 66, 23–33.
- Tiselius, P., Jonsson, P.R., and Verity, P.G., 1993. A model evaluation of the impact of food patchiness on foraging strategy and predation risk in zooplankton. *Bull. Mar. Sci.*, 53, 247–264.
- Tiselius, P., Jonsson, P.R., Karrtvedt, S., Olsen, E.M., and Jordstad, T., 1997. Effects of copepod foraging behavior on predation risk: an experimental study of the predatory copepod *Pareuchaeta norvegica* feeding on *Acartia clausi* and *A. tonsa* (Copepoda). *Limnol. Oceanogr.*, 42, 164–170.
- Titelman, J., 2001. Swimming and escape behavior of copepod nauplii: implications for predator–prey interactions among copepods. *Mar. Ecol. Prog. Ser.*, 213, 203–213.
- Tsonis, A.A. and Elsner, J.B., 1995. Testing for scaling in natural forms and observables. *J. Stat. Phys.*, 81, 869–880.
- Turchin, P., 1991. Translating foraging movements in heterogeneous environments into the spatial distribution of foragers. *Ecology*, 72, 1253–1266.
- Turchin, P., 1996. Fractal analysis of movement: a critique. *Ecology*, 77, 2086–2090.
- Turchin, P., 1998. *Quantitative Analysis of Movement*. Sinauer Associates, Sunderland, MA.
- Turchin, P., Odendaal, F.J., and Rausher, M.D., 1991. Quantifying insect movement in the field. *Environ. Entomol.*, 20, 955–963.
- Turner, M.G. and Gardner, R.H., 1991. Quantitative methods in landscape ecology: an introduction, in Turner, M.G. and Gardner, R.H., Eds., *Quantitative Methods in Landscape Ecology*. Springer-Verlag, New York, 3–14.
- Van Ballemberghe, V., 1983. Extraterritorial movements and dispersal of wolves in southcentral Alaska. *J. Mamm.*, 64, 168–171.
- van Duren, L.A. and Videler, J.J., 1995. Swimming behaviour of development stages of the calanoid copepod *Temora longicornis* at different food concentrations. *Mar. Ecol. Prog. Ser.*, 126, 153–161.
- van Duren, L.A. and Videler, J.J., 1996. The trade-off between feeding mate seeking and predator–prey avoidance in copepods: behavioural responses to chemical cues. *J. Plankton Res.*, 18, 805–818.
- Van Leeuwen, H.C. and Maly, E.J., 1991. Changes in swimming behavior of male *Diatomus leptotus* (Copepoda: Calanoida) in response to gravid females. *Limnol. Oceanogr.*, 36, 1188–1195.
- Voss, R.F., 1988. Fractals in nature: from characterization to simulation, in Peitgen, H.O. and Saupe, D., Eds., *The Science of Fractal Images*. Springer, New York, 21–70.
- Weissburg, M.J., Doall, M.H., and Yen, J., 1998. Following the invisible trail: kinematic analysis of mate tracking in the copepod *Temora longicornis*. *Philos. Trans. R. Soc. Long. B*, 353, 701–712.
- Wiens, J.A., 1989. Spatial scaling in ecology. *Funct. Ecol.*, 3, 385–397.
- Wiens, J.A. and Milne, B.T., 1989. Scaling of “landscapes” in landscape ecology, or landscape ecology from a beetle’s perspective. *Land. Ecol.*, 3, 87–96.
- Wiens, J.A., Crist, T.O., and Milne, B.T., 1993. On quantifying insect movements. *Environ. Entomol.*, 22, 709–715.
- Wiens, J.A., Crist, T.O., With, K.A., and Milne, B.T., 1995. Fractal patterns of insect movement in microlandscape mosaics. *Ecology*, 76, 663–666.
- Williamson, C.E., 1981. Foraging behavior of a freshwater copepod: frequency changes in looping behavior at high and low prey densities. *Oecologia*, 50, 332–336.
- Wilson, R.S. and Greaves, J.O.B., 1979. The evolution of the bugsystem: recent progress in the analysis of bio-behavioral data, in Jacoff, F.S., Ed., *Advances in Marine Environmental Research*. Proc. Symp. U.S. EPA (EPA-600/9-79-035), 252–272.
- With, K.A., 1994a. Using fractal analysis to assess how species perceive landscape structure. *Land. Ecol.*, 9, 25–36.
- With, K.A., 1994b. Ontogenetic shifts in how grasshoppers interact with landscape structure: an analysis of movement patterns. *Funct. Ecol.*, 8, 477–485.
- Wolk, F., Yamazaki, H., Seuront, L., and Lueck, R.G., 2002. A new free-fall profiler for measuring biophysical microstructure. *J. Atmos. Ocean. Tech.*, 19, 780–793.

- Wong, C.K., Ramcharan, C.W., and Sprules, W.G., 1986. Behavioral responses of a herbivorous copepod to the presence of other zooplankton. *Can. J. Zool.*, 64, 1422–1425.
- Wu, K.K.S., Lahav, O., and Rees, M.J., 1999. The large-scale smoothness of the Universe. *Nature*, 397, 225–230.
- Wu, H., Li, B.L., Springer, T.A., and Neill, W.H., 2000. Modelling animal movement as a persistent random walk in two dimensions: expected magnitude of the net displacement. *Ecol. Model.*, 132, 115–124.
- Yamazaki, H. and Squires, K.D., 1996. Comparison of oceanic turbulence and copepod swimming. *Mar. Ecol. Prog. Ser.*, 144, 299–301.
- Yen, J. and Strickler, J.R., 1996. Advertisement and concealment in the plankton: what makes a copepod hydrodynamically conspicuous? *Invert. Biol.*, 115, 191–205.
- Yen, J., Weissburg, M.J., and Doall, M.H., 1998. The fluid physics of signal perception by a mate-tracking copepod. *Philos. Trans. R. Soc. Lond. B*, 353, 787–804.
- Young, S. and Getty, C., 1987. Visually guided feeding behavior in the filter feeding cladoceran, *Daphnia magna*. *Anim. Behav.*, 35, 541–548.
- Young, S. and Taylor, V.A., 1990. Swimming tracks in swarms of two cladoceran species. *Anim. Behav.*, 39, 10–16.
- Zar, J.H., 1996. *Biostatistical Analysis*. Prentice-Hall International, Englewood Cliffs, NJ.

